Application of bioactive compounds on small-caliber vascular graft for prevention of intimal hyperplasia

Mi Hee Lee

Department of Medical Science

The Graduate School, Yonsei University

Application of bioactive compounds on small-caliber vascular graft for prevention of intimal hyperplasia

Mi Hee Lee

Department of Medical Science

The Graduate School, Yonsei University

Application of bioactive compounds on small-caliber vascular graft for prevention of intimal hyperplasia

Directed by Professor Jong-Chul Park

The Doctoral Dissertation's Thesis submitted to the Department of Medical Science, the Graduate School of Yonsei University in partial fulfillment of the requirements for the degree of Doctor of Philosophy

Mi Hee Lee

December 2010

This certifies that the Doctoral Dissertation's Thesis of Mi Hee Lee is approved.

These Supervisor : Jong-Chul Park

Thesis Committee Member #1 : Ki Dong Park

Thesis Committee Member #2 : Seung Jin Lee

Thesis Committee Member #3 : Jong-Won Ha

Thesis Committee Member #4 : Ki-Chul Hwang

The Graduate School
Yonsei University

December 2010

Acknowledgements

대학을 졸업하고 대학원이라는 또 다른 작은 사회에 발을 딛고 어느덧 7 년이라는 시간이 지난 지금, 처음 시작의 설렘과 두려움, 또한 다짐들을 되짚어 생각해 봅니다. 조금하게 지나갔던 2 년의 석사과정, 좌절과 도전을 반복한 4 년 반의 박사과정을 이제 마무리합니다. 아쉬움과 함께 학위과정 동안 많은 것을 느끼고, 많은 사람들을 만나고, 한 단계 성장하는 시간이었던 것 같습니다. 그 결과 부족하지만 작은 결실로 이 논문을 완성하였고, 저를 옆에서 지켜보아 주시며 끊임 없이 힘을 주신 분들께 이 작은 지면을 통해 감사의 마음을 전해드리고자 합니다.

부족한 저를 연구자의 길로 이끌어 주시고, 참된 연구자의 마음가짐과 삶에 대한 성실함의 가르침을 주신 박종철 교수님께 가장 먼저 감사의 마음을 전하고 싶습니다. 앞으로 시작되는 더 어려운 길에서 학문과 삶에 대한 교수님의 가르침을 잃지 않고 최선을 다해 살아가겠습니다. 바쁘신 데도 불구하고 연구에 많은 관심으로 연구방향과 과정에 많은 조언과 더불어 논문의 지도를 맡아주신 이화여대 이승진 교수님과 아주대학교의 박기동 교수님, 심장내과의 하종원 교수님, 심혈관 연구소의 황기철 교수님께 깊이 감사 드립니다.

항상 많은 관심과 사랑으로 가르침을 주시는 나노사업단의 이인섭교수님과 세종대학교의 이천용 교수님, 화학과의 김용록 교수님께도 감사 드립니다. 학위과정 동안 많은 보살핌을 주신 의학공학교실의 서활 교수님, 김덕원 교수님, 김남현 교수님, 유선국 교수님께도 감사의 마음을 전합니다. 어려운 동물실험에 대한 방향설정과 조언을 주신 흉부외과의 박한기 선생님, 내일처럼 함께 실험 해주시며 도와주신 장의화 선생님 정말 감사 드립니다.

7 년이라는 시간 동안 의학공학교실 일원으로 항상 함께 해준 세포제어연구실의 실험실원 모두에게 감사의 마음을 전하고 싶습니다. 많은 격려와 도움을 주시는 이동희 박사님, 실험에 대한 조언을 아끼지 않으신 박봉주 박사님, 세세한 것부터 큰 것까지 많은 조언을 주신 부산대 한동욱 교수님 감사합니다. 기쁠 때나 힘들 때나 함께 웃어주고 울어주었던 현숙 언니, 박사동기로 함께한 김정성 선생님(졸업 축하드려요!!), 연구에 열의가 멋진 한인호 박사님,

여성스럽지만 남모를 입맛의 소유자 학희언니(박사님), 학위를 위한 도전이 멋진 김동빈 선생님, 까칠하지만 속정 깊은 혜리, 언제나 밝은 재경이, 항상 든든하고 믿음직한 병주, 막둥이 통영아가씨 정현이, 하하맨 대형이, 새식구 현용이 (석사졸업 축하한다!!), 꽃다운 나이 여송이에게도 감사의 마음 전합니다. 멀리 싱가포르에 있지만 항상 옆에 있는 듯한 연이, 사회인으로 자리잡은 수창이, 멀리 독일에서 학문에 매진중인 아즘마 동정이, 영어교정으로 도와준 슬로바키아댁 박보라 Barbora Vagaska 등 모자란 선배 아래서 잘 버텨준 후배들에게 감사 드립니다.

학부시절 함께 불어 다니며, 함께한 아즘마 옥경이, 영원한 홍양 은정이, 엄마가 되는 설주 등 나의 친구들에게도 고마움과 미안함의 마음을 전합니다. 바쁘다는 핑계로 도와주지 못하는 나를 이해해주는 회장님 원진언니, 우진언니, 아들 낳느라 고생한 남희, 주영언니, 혜원엄마 진영이, 주일학교 선생님들과 친구들, 기도의 후원자이신 목사님과 엘림교회 가족들에게도 감사 드립니다.

부족하고 무뚝뚝한 딸을 언제나 믿어주시며 후원자로 30 년 동안 지켜주신 부모님, 어떤 말로도 표현 못할 정도로 감사 드리고 사랑합니다. 딸들 위해 더위와 추위에 고생하시는 아빠, 나이 많은 딸 위해 아침마다 도시락 준비하시는 엄마..부모님의 기대 저버리지 않은 딸 되겠습니다. 건강하세요.. 6 년차 어린이집 선생님 계희, RN 으로 첫 사회에 나간 계정이 에게도 고마운 마음을 전하며 멋지게 성장하자 동생들아…

마지막으로 힘들 때나 기쁠 때 언제나 위로해주시며 예비하시는 나의 하나님의 큰 사랑에 감사 드립니다. 앞으로 예비하신 길을 향해 따라가며 기도하고 준비하는 참된 예수님의 제자가 되도록 노력하겠습니다.

박사과정의 끝이자, 더 큰 세계로 향해 다시 시작하는 이 순간 염려와 사랑으로 도와주시는 모든 분들을 위해 노력하는 자 되겠습니다.

2010 년 12 월
이미희 드림

Table of contents

LIST OF FIGURES

Abstract

Application of bioactive compound on small-caliber vascular graft for prevention of intimal hyperplasia

Mi Hee Lee

Department of Medical Science
The Graduate School, Yonsei University

(Directed by Professor Jong-Chul Park)

Intimal hyperplasia is an excessive tissue ingrowths and a chronic structural lesion that is observed at a site of atherosclerotic lesion formation, arterial angioplasty, and vascular graft anastomoses etc. It is a result of the vessel wall's response to injury, and characterized by formation of a neointiml consisting of mainly attributable vascular smooth muscle cell (VSMC) migration and proliferation from the media to the intima and extracellular matrix remodeling. Dedifferented VSMCs of the media layers are phenotypically modulated from contractile state to the active synthetic state and induce proliferation and migration of VSMC from the media to the intima and extracellular matrix (ECM) protein deposition. Epigallocatechin 3-O-gallate (EGCG) and resveratrol have been exported to have antioxidant, anti-proliferative and anti-thrombogenic effect.

In this study, we investigate the effects of natural polyphenol, such as EGCG and resveratrol, on dedifferentiation, and the intracellular signal transduction pathway of PDGF-bb in rat aortic vascular smooth muscle cell and demonstrate the prevention mechanism of VSMC on intimal hyperplasia. Additionally, we prepare the polyphenol eluting biodegradable PLGA sheet for local delivery of polyphenol and investigate the effect of external application of polyphenol eluting biodegradable sheet on intimal hyperplasia after balloon injury of abdominal aorta in an experimental rabbit model.

10 ng/ml PDGF-bb induced a RAOSMC proliferation and cell vyvle progression. 10 ng/ml PDGF-bb treatments to serum starved RAOSMC induced phosphorylation of PDGFR-β after 10min incubation and maintained over 4h of stimulation on RAOSMC and led to a complete 42/44 MAPK phosphorylation which peaked within 30 min and returned to baseline levels at 120 min. Moreover, other intracellular signal pathways, phosphorylation of p38 MAPK and Akt, was activated by PDGF-bb stimulation. Treatment of EGCG with PDGF-bb significantly inhibited the proliferation of RAOSMC stimulated by dose dependently. Therefore, RAOSMC synchronized with EGCG inhibited proliferation stimulated by PDGF-bb stimulation. Treatment of 50 μM EGCG inhibited almost completely the growth of ROASMC. Also, cell cycle progression and MMP release in RAOSMC was inhibited by EGCG treatment whether stimulated with EGCG and PDGF-bb or stimulated with PDGF-bb after EGCG pretreatment. However, PDGF-bb stimulation on RAOSMC

starved with 50 μM EGCG was inhibited, as shown by decreased phosphorylation of PDGFR-β and intracellular signal cascade. Therefore, PDGF-bb stimulation with 50 μM EGCG on serum starved RAOSMC completely inactivated PDGFR-β phosphorylation. According to inactivation of PDGFR-β by EGCG, phosphorylation of 42/44 MAPK, p38 MAPK, and Akt was suppressed to baseline levels as in serum starved RAOSMC. In conclusion, EGCG inhibited RAOSMC dedifferentiation by interruption of PDGF-bb signal pathway, probably by directly binding with PDGF-bb and preventing PDGFR-b phosphorylation by incorporation into cell membrane.

Treatment of RAOSMC with resveratrol were significantly inhibited the PDGF-bb stimulated proliferation dose dependently. Also, treatment of 100 μM resveratrol inhibited almost completely the growth. In phenotype exchange in PDGF stimulation, serum starved RAOSMC maintained spindle morphology and aligned arrangement of actin filament, whereas PDGF-bb stimulated RAOSMC change form spindle to polygonal morphology and disassembled distribution of actin filaments. However, resveratrol treatment inhibited the phenotype change and disassembly of actin filament, and maintained the expression of contractile phenotype related protein such as calponin and smooth muscle actin–alpha. In addition, morphology of PDGF-bb stimulated RAOSMC exhibited greater circularity and area, compared with serum starved RAOSMC. Resveratrol inhibited the change of circularity and area stimulated by PDGF-bb. Phosphorylation of PDGFR-b decreased at 10min incubation with 10 ng/ml

PDGF-bb and 100 μM resveratrol, however it was similar with 10min incubation with only PDGF-bb stimulation. Similarly, resveratrol slightly inhibited phosphorylation of 42/44 MAPK and p38 MAPK. However, Akt and mTOR phosphorylation upon PDGF stimulation elicited a strong and detectable signal for several hours, while PDGF stimulation with resveratrol induced only weakly Akt phosphorylation. In conclusion, RAOSMC dedifferentiation, phenotype and proliferation rate were inhibited by resveratrol by interrupting the balance of the Akt and 42/44MAPK and p38MAPK pathway activation stimulated by PDGF-bb.

The electrospun PLGA fibers had typical fiber mat and a bead-free fibrous structure with wide range of fiber diameters whether in the presence or absence of EGCG or resveratrol. EGCG and resveratrol was encapsulated in PLGA fiber. EGCG and resveratrol eluting PLGA sheet appeared a red and yellow color, respectively. From the FTIR spectra, distinctive peaks of EGCG and resveratrol were observed from spectra of their respective EGCG or resveratrol eluting PLGA sheet. This indicated that EGCG or resveratrol were well loaded and dispersed into PLGA sheets. The EGCG and resveratrol loading efficiencies on EGCG and resveratrol eluting PLGA sheet were found to be 80~90 % of input amount for sheet fabrication. Each polyphenol release profiles are shown to be different for EGCG and resveratrol. In case of EGCG there was burst diffusion at 1 day followed by sustained release up to 40 days from EGCG eluting PLGA sheets. Resveratrol was released in a logarithmic manner up to 20 days after

which the release rate decreased with time. We investigated the effect of externally wrap with EGCG and resveratrol eluting PLGA sheet in balloon injury aorta of rabbit. Morphometric analysis revealed significantly decreased intima/media (I/M) ratio in EGCG eluting electrospun PLGA fiber sheet. We found a significantly ($p<0.05$) 30% and 50% reduction of intimal area in wrapped aorta with EGCG and resveratrol. The medial area was not significantly by EGCG and resveratrol treatment in comparison with vehicle PLGA control.

From the therapeutic point of view, these results suggest that EGCG and resveratrol can be a potential agent for the prevention of VSMC dedifferentiation and their local release from electrospun PLGA fiber sheet can be applicable as a method to prevent intimal hyperplasia in stent, catheter, and vascular bypass and graft.

Key words : Vascular smooth muscle cell, Epigallocatechin-3-O-gallate, Resveratrol, Platelet-derived growth factor-bb, Platelet-derived growth factor receptor-β, Dedifferentiation, Intracellular signaling pathways, Intimal hyperplasia, Electrospun, drug delivery system

Application of bioactive compound on small-caliber vascular graft for preventing intimal hyperplasia

Mi Hee Lee

Department of Medical Science
The Graduate School, Yonsei University

(Directed by Professor Jong-Chul Park)

I. INTRODUCTION

1. Intimal hyperplasia

Cardiovascular disease, including coronary artery and peripheral vascular disease, are increasing with the increase of aging population and dietary change. Cardiovascular disease is a major cause of mortality and morbidity. Modern therapies are routine performed to treat of these diseases, such as percutaneous transluminla coronary angioplasty (PTCA)[1] atheroctomy[2], stent placement[3], and implantation of vascular graft [4,5]. However, recurrent resetnosis is the major complication of their long-term success with revascularization procedures and has remained a critical concern by aconstriction or renarrowing of the arteries at the site of the treatment. The primary mechanism of failure of these revascularization and interventional procedures is intimal hyperplasia (IH).

The artery walls consist of three layers distinct layers; the intima, the media and the adventitia. The intimal layer consists of a layer of endothelial cells (EC) lying on a connective tissue layer known as the internal elastic lamina (IEL). The IEL is composed of type IV collagen, laminin and heparin sulfate proteoglycans. The medial layer is composed of vascular smooth muscle cells (VSMC) and extracellular matrix (ECM), which contains types I and III collagen, fibronectin, and chondroitin/dermatan sulphate proteoglycans. The medial layer is supported by another layer of connective tissue, the external elastic lamina (EEL) contained hydrophobic protein elastin. The Outer adventitia layer contains fibroblasts and fat cells in a loose connective tissue. (Fig. 1-1) [6,7]

The maintenance of vascular wall homeostasis requires a complex interplay between the major cellular components of the vessel wall, EC and VSMC. Major initiation of renarrowing at the site of the vascular treatment is vascular injury induced by stent implantation and vascular surgery. Endothelium is important factor to prevent vascular disease and performs important functions, which is a diffusion barrier to prevent plasma macromolecules from penetrating the vascular wall and displays a spectrum of biologic activities, such as the provision of an antithrombogenic surface, the focal metabolism, and substances production and release for regulation of vascular tone [8].

Intimal hyperplasia signifies an increase in the number of cells and the amount of ECM and these induce the more intimal thickening. Physiologically

mechanisms of intimal hyperplasia is broadly classified into (a) endothelium denude (b) platelet activation and events at the platelet surface (c) SMC migration and proliferation (d) remodeling of ECM (Fig. 1-2) [9,10].

Endothelium denude is occurred at the earliest response to injury and determined to degree of intimal damage. Vascular injury disrupts vascular integrity and damage of endothelial layer. Therefore, vessels are exposed to a greater shear stress into the arterial circulation.

Endothelium injury exposes the luminal surface of media and leads to platelet adhesion and aggregation at injury site and occasionally thrombus formation injury and occasionally thrombus formation. Activated platelets express many pro-inflammatory mediators, upregulate expression of cell adhesion molecules, release angiogenic growth factors, and promote leukocyte recruitment

These molecules, P-selectin, alpha granule adhesion molecule, and glycoprotein Iba, bind to circulating leukocytes by the platelet receptors P-selectin glycoprotein ligand (PSGL) and leads to leukocytes activation. The activated platelets also release numerous bioactive substances. These include enzymes such as matrix metalloproteinases (MMPs) and thrombin, growth factors such as basic fibroblast growth factor (FGF-2), transforming growth factor-β (TGF-β), platelet-derived growth factors (PDGFs), insulin growth factor-1 (IGF-1), and cytokines such as tumor necrosis factor-α (TNF-α) and interleukin-1 (IL-1), IL-6 and IL-8.[11,12] These mediators participate in the activation and phenotypic switch of VSMC, which results in VSMC migration and proliferation from the

media to the intimal layers. Then, ECM amounts, proteoglycans and hyaluronan etc., are synthesized by SMCs increase and participate in regulation of vascular permeability, lipid metabolism and thrombosis. After all, intimal layer is thickness and narrowing and consists of VSMC, ECM and macrophages.

Over the years, various experiments and efforts is performed to prevent or inhibit intimal hyperplasia. These include systemic pharmacological therapy, brachytherapy and stent, etc. Such therapeutic investigations have included antiplatelet agents (eg, aspirin), vasodilators (eg, calcium channel blockers), anticoagulants (eg, heparin), anti-inflammatory agents (eg, corticosteroids), agents to prevent vascular smooth muscle cell proliferation (eg, colchicine), and promoters of re-endothelization (eg, vascular endothelial growth factor). To overcome limitation of bare metal stent, a novel alternative strategy involves the use of a drug eluting stent with immunosuppressive or anti-proliferative drug. Although the outcomes have improved with refinements in surgical techniques and discovery of new pharmacological agents during the past two decades, long-term patency remains a significant concern for vascular surgeons.

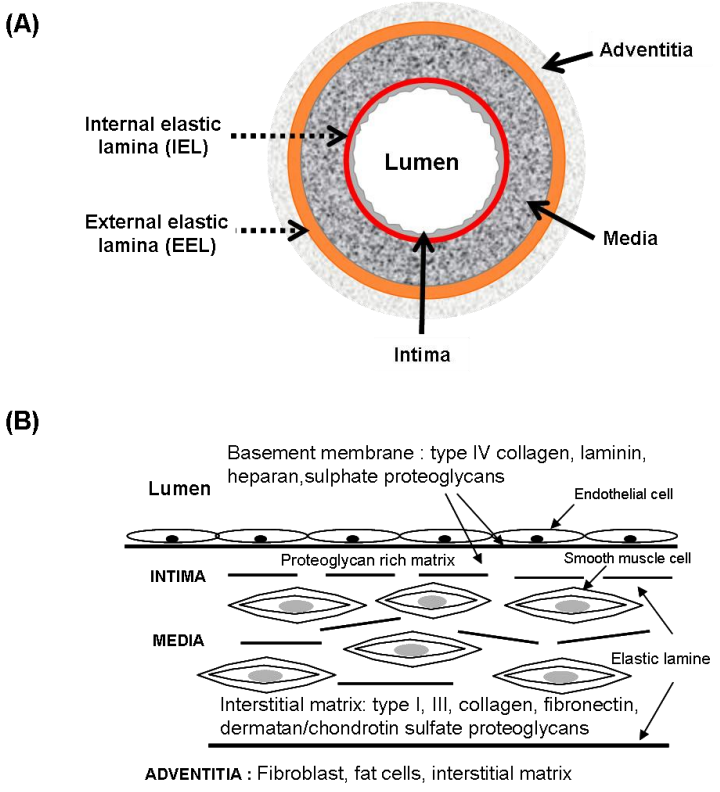

Figure 1-1. Schematic illustration of the structural characteristics of the normal arterial wall.

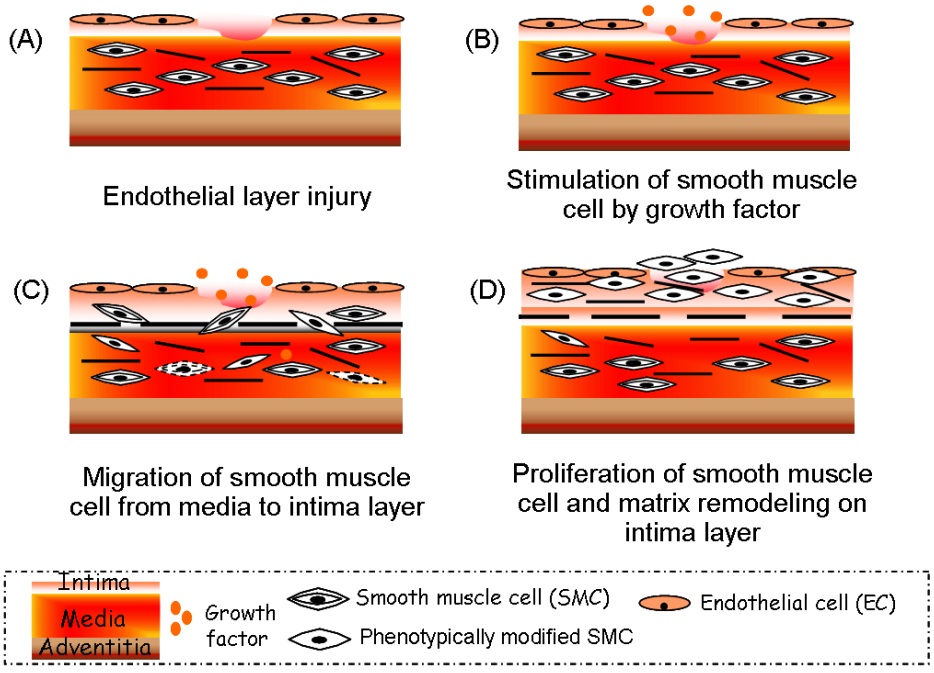

Figure 1-2. Mechanisms of intimal hyperplasia. (A) Endothelium denude, which triggers a cascade of events, including the recruitment of leukocytes. (B) Activation of vascular smooth muscle cells (VSMC) by cytokines and growth factors derived from platelets (C) Migration of VSMC from the media into neointima (D) Proliferation of VSMC and synthesis of extracellular matrix components on the luminal side of the vessel wall

2. Differentiation of vascular smooth muscle cell

Alternations of VSMC in the differentiated state to the de-differentiated (activation) state are important event in the pathogenesis of a variety of cardiovascular disease. VSMC is very little migratory and proliferative and retain the ability to quiescent, contractile phenotype in media layer in normal and mature vessels. VSMC has the primary function of contraction and exhibit a contractile phenotype by the expression of contractile markers specific to smooth muscle, such as smooth muscle myosin heavy chain (SM-MHC), SM α-actin (αSMA), h-caldesmon, and calponin[13~15].

Upon various stimuli as vascular injury and damage, VSMCs dedifferentiate and undergo rapid and quite phenotype modulation, which demonstrate increased rate of migration and proliferation to the intima, and synthesis of extracellular matrix, and at the same time, demonstrate a decrease in expression of SM-specific contractile markers[16~18]. Stimuli component released by vascular injury such as thrombin, PDGFs, FGG-2, TGF-β, and MMPs depend on the intracellular signaling operated by the mitogen-activated protein kinases (MAPK) for their biological functions[19,20].

Thus understanding of downstream signaling pathways and regulation of VSMC differentiation may contribute to therapeutic strategies for prevention and reduction of the development of intimal hyperplasia.

3. Drug delivery system using electrospun method

Local drug delivery systems have potential advantages, because they improve treatment and patient compliance, provide optimized drug concentration on site over prolong periods and reduce undesired side effects of the drug [21-23].

Degradable polymers have been widely explored in drug delivery study. Polymer using drug delivery systems are able to control and prolong drug release by adjusting the degradation rate of the polymer [24,25]. These polymers encapsulate different types of drug and have regulated to release pattern of drug [26-29]. Therefore, these allows for the development of various systems such as implants, pastes, hydrogels, film, and/or micro/nanoparticles, and other specific devices to deliver a particular medicine.

Aliphatic polyesters such as poly (D,L-lactide) (PLA) and its copolymers with glycolic acid (PLGA) are biodegradable and biocompatible polymers with remarkably broad applications in sustained drug delivery [30-32]. Nanofibers for drug release systems mainly come from biodegradable polymers, such as PLA[33], PCL[34-36], poly(D-lactide)(PDLA)[37], PLLA[38-40], PLGA[41-42], and hydrophilic polymers, such as PVA[43-45], PEG[44,46] and PEO[47]. Non-biodegradable polymers, such as PEU[48], were also investigated. Model drugs that have been studied include water soluble[33,37,39], poor-water soluble[46,48-52] and water-insoluble drugs [34,37,53,54]. The release of macromolecules, such as DNA[41] and bioactive proteins[47,55-58], from nanofibers was also investigated.

In recent year, the formation of fibers by electrospining has increasingly

become important in biomedical applications including tissue engineering, wound healing, and drug release[59,60]. Electrospining have basically three components; a high voltage supplier, a capillary tube with a pipette or needle of small diameter, and a metal collecting screen. Electrospining produce nanoscale and microscale polymeric fibers with high surface area-to-volume ratio and porosity between a spinneret and a grounded collector by high voltage source. When the electrostatic charge exceeds the surface tension of the solution, the fiber jet travels from the syringe nozzle to the electrically charged ground collector and allows the solvent to evaporate, thus leading to the deposition of the non-woven solid polymer fiber on the surface of the metallic target collector [59,61]. Electrospun fibers have exhibited many advantages as a potential drug delivery. The drug loading is very easy to implement in electrospinning process, and the high applied voltage had little influence on the drug activity. The high specific surface area and short diffusion passage length give the nanofiber drug system higher overall release rate than the bulk material (e.g. film). The release profile can be finely controlled by modulation of nanofiber morphology, porosity and composition into different shapes [57,58]. Furthermore, the physical/chemical properties of the electrospun nanofibers can be readily modified by encapsulation and/or immobilization of bio-active species to elicit specific biological responses and fibers may be suitable carriers for drug delivery.

4. Reference

1. Kearney M, Pieczek A, Haley L, Losordo DW, Andres V, Schainfeld R, et al. Histopathology of in-stent restenosis in patients with peripheral artery disease. Circulation 1997;95(8):1998-2002.
2. Marek JM, Koehler C, Aguirre ML, Westerband A, Gentile AT, Mills JL, et al. The histologic characteristics of primary and restenotic carotid plaque. J Surg Res 1998;74(1):27-33.
3. Hoffman R, Mintz GS, Dussaillant GR, Popma JJ, Pichard AD, Satler LF et al. Patterns and mechanisms of instent restenosis: a serial intravascular ultrasound study. Circulation 1996; 94:1247–54.
4. Goldman S, Zadina K, Moritz T, Ovitt T, Sethi G, Copeland JG. et al. Long-term patency of saphenous vein and left internal mammary artery grafts after coronary artery bypass surgery: results from a Department of Veterans Affairs Cooperative Study. J Am Coll Cardiol 2004;44: 2149–2156.
5. Ascher E, Gade P, Hingorani A, Mazzariol F, Gunduz Y, Fodera M. et al. Changes in the practice of angioaccess surgery: impact of dialysis outcome and quality initiative recommendations. J Vasc Surg 2000;31: 84–92.
6. Stary HC. The sequence of cell and matrix changes in atherosclerotic lesions of coronary arteries in the first forty years of life. Eur Heart J 1990; 11 (Suppl E): 3–19.

7. Wight T. The extracellular matrix and atherosclerosis. Curr Opin Lipidol 1995; 6: 326–34.
8. Patel SD, Waltham M, Wadoodi A, Burnand KG, Smith A. The role of endothelial cells and their progenitors in intimal hyperplasia. Ther Adv Cardiovasc Dis 2010;4(2):129-41.
9. Davies MG, Hagen PO. Pathophysiology of vein graft failure: a review. Eur J Vasc Endovasc Surg 1995;9: 7–18.
10. Scott NA. Restenosis following implantation of bare metal coronary stents: Pathophysiology and pathways involved in the vascular response to injury. Adv Drug Deliv Rev 2006;58: 358–76.
11. Newby AC, Zaltsman AB. Molecular mechanisms in intimal hyperplasia. J Pathol. 2000;190(3):300-9.
12. Mitra AK, Gangahar DM, Agrawal DK. Cellular, molecular and immunological mechanisms in the pathophysiology of vein graft intimal hyperplasia. Immunol Cell Biol 2006;84(2):115-24.
13. Kawai-Kowase K., Owens1 GK. Multiple repressor pathways contribute to phenotypic switching of vascular smooth muscle cells. Am J Physiol Cell Physiol 2007;292:C59–C69.
14. Kim S, Ip HS, Lu MM, Clendenin C, Parmacek MS. A serum response factor-dependent transcriptional regulatory program identifies distinct smooth muscle cell sublineages. Mol Cell Biol 1997;17: 2266–78.
15. Gualberto A, LePage D, Pons G, Mader SL, Park K, Atchison ML, et al.

Functional antagonism between YY1 and the serum response factor. Mol Cell Biol 1992;12: 4209–14.

16. Owens GK. Regulation of differentiation of vascular smooth muscle cells. Physiol Rev 1995;75:487-517.
17. Owens GK, Kumar MS, Wamhoff BR. Molecular regulation of vascular smooth muscle cell differentiation in development and disease. Physiol Rev 2004;84:767-801.
18. Sobue K, Hayashi K, Nishida W. Expressional regulation of smooth muscle cell-specific genes in association with phenotypic modulation. Mol Cell Biochem 1999;190:105-18.
19. Rzucidlo EM, Martin KA, Powell RJ. Regulation of vascular smooth muscle cell differentiation. J Vasc Surg. 2007;45 Suppl A:A25-32.
20. Yu PJ, Ferrari G, Pirelli L, Gulkarov I, Galloway AC, Mignatti P, et al. Vascular injury and modulation of MAPKs: a targeted approach to therapy of restenosis. Cell Signal 2007;19(7):1359-71.
21. Jagur-Grodzinski, J. Polymers for targeted and/or sustained drug delivery. Polym Adv Technol 2009; 20:595–606.
22. Kim S, Kim JH, Jeon O, Kwon IC, Park K. Engineered polymers for advanced drug delivery. Eur J Pharm Biopharm 2009;71(3):420-30.
23. Musthaba SM, Baboota S, Ahmed S, Ahuja A, Ali J. Status of novel drug delivery technology for phytotherapeutics. Expert Opin Drug Deliv 2009;6(6):625-37.

24. Maretschek S, Greiner A, Kissel T. Electrospun biodegradable nanofiber nonwovens for controlled release of proteins. J Control Release 2008;127(2):180-7.

25. Singh S, Webster DC, Singh J. Thermosensitive polymers: synthesis, characterization, and delivery of proteins. Int J Pharm 2007;341(1-2):68-77.

26. Uhrich KE, Cannizzaro SM, Langer RS, Shakesheff KM. Polymeric systems for controlled drug release. Chem Rev 1999;99(11):3181-98.

27. Mundargi RC, Babu VR, Rangaswamy V, Patel P, Aminabhavi TM. Nano/micro technologies for delivering macromolecular therapeutics using poly(D,L-lactide-co-glycolide) and its derivatives. J Control Release 2008;125(3):193-209.

28. Ganta S, Devalapally H, Shahiwala A, Amiji M. A review of stimuli-responsive nanocarriers for drug and gene delivery. J Control Release 2008;126(3):187-204.

29. LaVan DA, McGuire T, Langer R. Small-scale systems for in vivo drug delivery. Nat Biotechnol 2003;21(10):1184-91.

30. Guo XD, Zhang LJ, Qian Y, et al. Effect of composition on the formation of poly(DL-lactide) microspheres for drug delivery systems: Mesoscale simulations. Chem Eng J 2007; 131(1-3):195-201.

31. Budhian A, Siegel SJ, Winey KI. Haloperidol-loaded PLGA nanoparticles: systematic study of particle size and drug content. Int J Pharm 2007;336(2):367-75.

32. Katti DS, Robinson KW, Ko FK, Laurencin CT. Bioresorbable nanofiber-based systems for wound healing and drug delivery: optimization of fabrication parameters. J Biomed Mater Res Part B 2004;70B:286-96.
33. Kenawy E-R, Bowlin G L, Mansfield K, Layman J, Simpson DG, Sanders EH, et al. Release of tetracycline hydrochloride from electrospun poly(ethylene-co-vinylacetate), poly(lactic acid), and a blend. J Contr Rel 2002; 81(1-2):57-64.
34. Zhang YZ, Feng Y, Huang ZM, Ramakrishna S, Lim CT. Fabrication of porous electrospun nanofibres. Nanotechnology 2006; 17(3):901-8.
35. Luong-Van E, Grondahl L, Chua K N, Leong KW, Nurcombe V, Cool SM. Controlled release of heparin from poly(e-caprolactone) electrospun fibers. Biomaterials 2006;27(9): 2042-50.
36. Jiang H, Hu Y, Zhao P, Li Y, Zhu K. Modulation of protein release from biodegradable core shell structured fibers prepared by coaxial electrospinning. J Biomed Mater Res Part B: Appl Biomater 2006;79B(1): 50-7.
37. Zong X, Kim K, Fang D, Ran S, Hsiao BS, Chu B. Structure and process relationship of electrospun bioabsorbable nanofiber membranes. Polymer 2002;43(16): 4403-12.
38. Zeng J, Xu X, Chen X, Liang Q, Bian X, Yang L, et al. Biodegradable electrospun fibers for drug delivery. J Contr Rel 2003;92(3):227-31.
39. Xu X, Yang L, Xu X, Wang X, Chen X, Liang Q, et al. Ultrafine

medicated fibers electrospun from W/O emulsions. J Contr Rel 2005;108(1):33-42.

40. Qi H, Hu P, Xu J, Wang A. Encapsulation of drug reservoirs in fibers by emulsion electrospinning: morphology characterization and preliminary release assessment. Biomacromolecules 2006;7(8):2327-30.
41. Luu YK, Kim K, Hsiao BS, Chu B, Hadjiargyrou M. Development of a nanostructured DNA delivery scaffold via electrospinning of PLGA and PLA-PEG block copolymers. J Contr Rel 2003;89(2):341-53.
42. Kim K, Luu Y K, Chang C, Fang D, Hsiao BS, Chu B, et al. Incorporation and controlled release of a hydrophilic antibiotic using poly(lactide-co-glycolide)-based electrospun nanofibrous scaffolds. J Contr Rel 2004;98(1):47-56.
43. Taepaiboon P, Rungsardthong U, Supaphol P. Drug-loaded elec-trospun mats of poly(vinyl alcohol) fibres and their release charac-teristics of four model drugs. Nanotechnology 2006;17(9):2317-29.
44. Yang D, Li Y, Nie J. Preparation of gelatin/PVA nanofibers and their potential application in controlled release of drugs. Carbohydr Polym 2007;69(3):538-43.
45. Kenawy E-R, Abdel-Hay FI, El-Newehy MH, Wnek GE. Controlled release of ketoprofen from electrospun poly(vinyl alcohol) nanofibers. Mater Sci Eng A: Struct Mater Prop Microstruct Proc 2007;A459(1-2):390-6.

46. Jiang H, Fang D, Hsiao B, Chu B, Chen W. Preparation and characterization of ibuprofen-loaded poly(lactide-co-glycolide)/poly (ethylene glycol)-g-chitosan electrospun membranes. J Biomater Sci Polym Ed 2004;15(3): 279-96.
47. Kim TG, Lee DS, Park TG. Controlled protein release from electrospun biodegradable fiber mesh composed of poly(e-caprolactone) and poly(ethylene oxide). Int J Pharm 2007;338(1-2):276-83.
48. Verreck G, Chun I, Rosenblatt J, Peeters J, Dijck AV, Mensch J, et al. Incorporation of drugs in an amorphous state into electrospun nanofibers composed of a water- insoluble, nonbiodegradable polymer. J Contr Rel 2003;92(3):349-60.
49. Verreck G, Chun I, Peeters J, Rosenblatt J, Brewster ME. Preparation and characterization of nanofibers containing amorphous drug dispersions generated by electrostatic spinning. Pharm Res 2003;20(5):810-7.
50. Cui W, Li X, Zhu X, Yu G, Zhou S, Weng J. Investigation of drug release and matrix degradation of electrospun poly(DL-lactide) fibers with paracetanol inoculation. Biomacromolecules 2006;7(5):1623-9.
51. Xie J, Wang C. Electrospun micro- and nanofibers for sustained de-livery of paclitaxel to treat C6 glioma in vitro. Pharm Res 2006;23(8):1817-26.
52. Wang M, Wang L, Huang Y. Electrospun hydroxypropyl methyl cel-lulose phthalate (HPMCP)/erythromycin fibers for targeted release in intestine. J Appl Polym Sci 2007;106(4):2177-84.

53. Tungprapa S, Jangchud I, Supaphol P. Release characteristics of four model drugs from drug-loaded electrospun cellulose acetate fiber mats. Polymer 2007;48(17):5030-41.

54. Pornsopone V, Supaphol P, Rangkupan R, Tantayanon S. Electrospun methacry-late-based copolymer/indomethacin fibers and their release characteristics of indomethacin. J Polym Res 2007;14(1):53-9.

55. Zeng J, Aigner A, Czubayko F, Kissel T, Wendorff JH, Greiner A. Poly(vinyl alcohol) nanofibers by electrospinning as a protein delivery system and the retardation of enzyme release by additional polymer coatings. Biomacromolecules 2005;6(3): 1484-8.

56. Chunder A, Sarkar S, Yu Y, Zhai L. Fabrication of ultrathin polyelectrolyte fibers and their controlled release properties. Coll Surf B: Biointerf 2007; 58(2):172-9.

57. Jiang H, Hu Y, Li Y, Zhao P, Zhu K, Chen W. A facile technique to prepare biodegradable coaxial electrospun nanofibers for controlled release of bioactive agents. J Contr Rel 2005;108(2-3):237-43.

58. Chew SY, Wen J, Yim EKF, Leong KW. Sustained release of proteins from electrospun biodegradable fibers. Biomacromolecules 2005;6(4): 2017-24.

59. Kidoaki S, Kwon IK, Matsuda T. Mesoscopic spatial designs of nano- and microfiber meshes for tissue-engineering matrix and scaffold based on newly devised multilayering and mixing electrospinning techniques.

Biomaterials 2005;26(1):37-46.

60. Chen JP. Chang GY. Chen JK. Electrospun collagen/chitosan nanofibrous membrane as wound dressing. Colloids Surf A Physicochem Eng Asp 2007;313:183-8.

61. Sill TJ, von Recum HA. Electrospinning: applications in drug delivery and tissue engineering. Biomaterials 2008;29(13):1989-2006.

II. DEDIFFERENTIATION OF VASCULAR SMOOTH MUSCLE CELL STIMULATED BY PLATELET DERIVED GROWTH FACTOR-BB IS INHIBITED BY BLOCKING OF INTRACELLULAR SIGNALING BY EPIGALLOCATECHIN-3-O-GALLATE

1. Introduction

Several vascular diseases involve vascular smooth muscle cell (VSMC) proliferation as their primary mechanism. De-differented VSMCs induce proliferation and migration of VSMC and extracellular matrix (ECM) protein deposition [1-4]. Intimal hyperplasia is an excessive tissue ingrowth and chronic structural lesion that can be observes at the site of atherosclerotic lesion formation, arterial angioplasty, vascular graft anastomoses, etc. It is a result of the vessel wall's response to injury and is characterized by formation of a neointimal consisting of mainly attributable VSMC migration and proliferation from the media to the intima and extracellular matrix remodeling [5-6]. Vascular proliferation is the most important factor in intimal hyperplasia and is linked to other cellular processes such as migration, inflammation and extracellular matrix production.

Platelet-derived growth factor-bb (PDGF-bb) is one of the most potent mitogens and chemoattractants for VSMC and plays a central role via simultaneous interactions between them[7]. PDGF-bb induced dedifferentiation and the MMP-2 upregulation[8,9] and migration[10] on VSMC. PDGF-bb binds to the PDGR

receptor (PDGFR)-β and subsequently activates several intracellular signaling cascades, including the extracellular signal–regulated kinase (ERK or p42/44 MAPK), p38 mitogen–activated protein kinase (p38 MAPK) pathways, and phosphatidylinositol 3-kinase-Akt (PI3K-Akt), and stimulates VSMC dedifferentiation [11].

Epigallocatechin gallate (EGCG) is most prevalent polyphenol contained in green tea. These have been reported to have antioxidant, anti-proliferative and anti-thrombogenic effect. Recent experiments have suggested that green tea cathechins reduce artherosclerotic lesions in various animal models and can prevent cardiovascular diseases [12-14]. EGCG inhibits VSMC invasion by preventing matrix metalloproteinase (MMP) expression, and provides a protective effect against atherosclerosis and cancer via matrix degradation [15].

In this study, we investigated the effects of EGCG on proliferation, cell cycle and the intracellular signal transduction pathway of PDGF-bb in rat aortic vascular smooth muscle cell (RAOSMC) and demonstrate the prevention mechanism of PDGF-bb stimulated RAOSMC dedifferentiation.

2. Materials and Methods

A. Cell Culture

RAOSMC were purchased from Biobud (Seoul, Korea) and used between passages 5 and 9. The cells were routinely maintained in Dulbecco's modified Eagles medium (Gibco, Carlsbad, CA, USA), supplemented with 10% fetal bovine serum (Sigma, St. Louis, MO, USA) and a 1% antibiotic-antimycotic solution containing 10,000 units penicillin, 10 mg streptomycin, and 25 μg amphotericin B per ml (Sigma) at 37℃ in a humidified atmosphere of 5% CO_2.

B. Cell Stimulation by PDGF-bb

For the experiment, RAOSMC were routinely seeded at a density of 5×10^4 cells/cm^2 and incubated for 24 h. The cells were synchronized in serum free DMEM medium for 24 h prior to the experiments. EGCG, the major polyphenolic constituent of green tea, was purchased from DSM Nutritional Products Ltd. It was dissolved in 50% DMSO (Sigma) for a stock solution of 100 mM and then diluted to the desired concentrations with media prior to cell treatment. The cells were preincubated with EGCG in starvation medium for 24 h and stimulated with serum free media containing 10 ng/ml human recombinant PDGF-bb (Sigma) in RAOSMC preincubated with EGCG. On the other hand, cells were synchronized in serum free DMEM medium for 24h and simulated with 10 ng/ml PDGF-bb containing EGCG for the desired time to

assess directly effect of PDGF-bb by EGCG on RAOSMC.

C. Cell Proliferation and DNA synthesis

Cell proliferation was determined by MTT assay [reduction of 3-(4,5-dimethylthiazol-2-yl)-2,5-diphenyltetrazolium bromide to a purple formazan product, Sigma] and a 5-bromo-2'-deoxyuridine (BrdU) incorporation assay (Roche applied science, Basel, Switzerland).

For the MTT assay, the cells were incubated with 0.5 mg/ml of MTT in the last 4 h of the culture period tested at 37 ℃ in the dark. The media were decanted and the produced formazan salts were dissolved with dimethylsulphoxide, and absorbance was determined at 570 nm by an automatic microplate reader (Spectra Max 340, Molecular Devices, Inc., Sunnyvale, CA, USA).

For BrdU incorporation assay, BrdU-labeling solution was added to the cells, which were then reincubated the cell for 2 h at 37 ℃. Labeling medium was then removed and the cells were incubated with fixation solution for 30 min at room temperature. After fixation of the cells, anti-BrdU-POD working solution was added and the cells were incubated for 90 min at room temperature. Then, the substrate solution was added and absorbance was measured at 370 nm with 492 nm reference wavelength by an automatic microplate reader (Spectra Max 340, Molecular Devices, Inc.).

D. Cell Cycle Analysis

To analyze the cell cycle, RAOSMC were collected and washed with cold phosphate-buffered saline (PBS, pH 7.2). The cells were resuspended in 95% cold methanol for 1 h at 4oC and then centrifuged at 120 xg for 5 min. The resultant pellet was washed twice with cold PBS and incubated with RNase A (20 U/ml final concentration, Sigma) at 37℃ for 30 min. Intracellular DNA was labeled with 100 μg/ml propidium iodide (PI, Sigma) for 1 h and then analyzed with a fluorescence-activated cell sorter (FACSCalibur, Becton Dickinson, San Jose, CA, USA). The cell cycle profile was gained by analyzing at least 20,000 cells with the ModFit© LT program written by Mac-App (Becton Dickinson).

E. Gelatin zymography

Gelatinase activity was detected in the conditioned medium of cultured RAOSMC. The conditioned media mixed with laemmli-buffer under non-reducing conditions were loaded onto 10% SDS-polyacrylamide gel containing 0.1% gelatin. After electrophoresis, the gels were washed for 20 min at room temperature in 2.5 % Triton X-100 and incubated for 18 h at 37℃ with reaction buffer 50mM Tris base (pH 7.6), 0.2M NaCl, 5mM CaCl2, 0.02% Brij 35). The gels were stained with Coomassie Brillant Blue R-2500 (0.1%) and destained. Densitometric analyses were performed with imageJ software (National Institutes of Health, Bethesda, MD, USA)

F. Western Blot analysis

After simulated with PDGF-bb, the cells were washed twice with cold PBS (10 mM, pH 7.4). Ice-cold RIPA lysis buffer (Santa Cruz Biotechnology Inc., Santa Cruz, CA, USA) was added to the cells for 5 min. The cells were scraped, and the lysate was cleared by centrifugation at 14,000 × g for 20 min at 4 ℃. The resultant supernatant (total cell lysate) was collected. Protein concentration was determined using a DC Bio-Rad assay kit (Bio-Rad Laboratories, Inc., Hercules, CA, USA). For immunoblot analysis, the protein was run on SDS-PAGE and then electrotransferrred onto a PVDF membrane. The membrane was blocked with blocking buffer (5% nonfat dry milk and 1% Tween-20 in 20 mM TBS, pH 7.6) for 1 h at room temperature and then probed overnight with phosphor PDGFR- β (pPDGFR-β), PDGFR-β, phosphor MEK1/2 (pMEK1/2), phosphor p42/44MAPK(pp42/44MAPK), phosphor Akt (pAkt), and phosphor p38MAPK (pp38MAPK) used at 1:1,000 dilution from Cell Signaling Technology (Danvers, MA, USA). Detection of horseradish peroxidase-conjugated secondary Ab (e.g., anti-rabbit IgG (1:5,000), anti-mouse IgG (1:2,000) from Santa Cruz Biotechnology Inc.) was accomplished using enhanced chemiluminescence using the ECL Plus detection kit (Amersham Biosciences, Buckinghamshire, England). Densitometric analyses were performed with imageJ (NIH)

G. Statistical Analysis

All variables were tested in three independent cultures for each experiment. The results are reported as a mean ± SD and compared to non-treated controls. Statistical analysis was performed using a one-way (ANOVA), followed by a Tukey HSD test for multiple comparisons using SPSS software. A p value of < 0.05 was considered statistically significant.

3. Results

A. Inhibitory effect of proliferation by PDGF-bb on EGCG preincubated RAOSMC

To investigate proliferation by PDGF-bb stimulation on RAOSMC preincubated with EGCG, increasing EGCG concentration was treated with serum free DMEM for 24 h at 70~80 % confluence RAOSMC. Cells were then washed twice with PBS and incubated with 10 ng/ml PDGF-bb for 24 h. 10 ng/ml PDGF-bb induced significant ($p < 0.05$) RAOSMC proliferations as compared with to the non-stimulated group as assessed by increased DNA synthesis and increased formazen absorbance. When cells were preincubated with increasing concentrations of EGCG, cell proliferation by 10 ng/ml PDGF-bb decreased in a significant ($p < 0.05$) dose-dependent manner of EGCG. Therefore, cell viability (Fig. 2-1A) and DNA synthesis (Fig. 2-1B) were not significantly induced in concentrations up to 50 μM. To investigate the effects of EGCG pretreatment on cell cycle distribution, DNA cell cycle analysis was performed on RAOSMC stimulated with PDGF-bb. As shown in Fig. 2-1C, EGCG pretreatment resulted in an appreciable increase in cells in the G0/G1-phase, with a decrease in S-phase cells in up to 20 μM EGCG pretreatment. These results indicate that EGCG pretreatment can suppress cell cycle progression and cell growth on RAOSMC with distributed PDGF-bb stimulation.

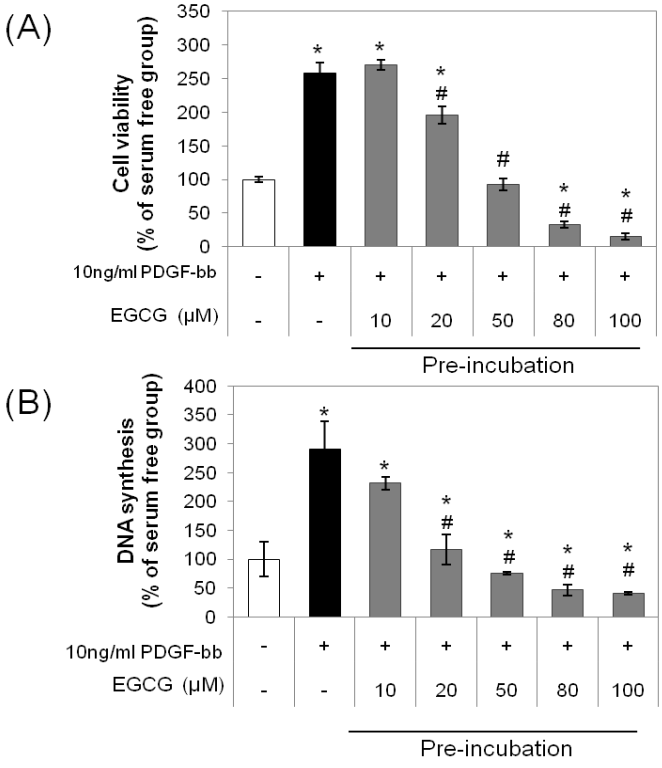

Figure 2-1. Anti-proliferative activity and cell cycle arrest activity by PDGF-bb on EGCG preincubated RAOSMC. After 24 h of starvation with DMEM containing increasing concentrations (10 – 80 μM) of EGCG, cells at 80% confluence were washed and treated with 10ng/ml PDGF-b. (A) The effects of growth inhibition on PDGF-bb stimulation in EGCG pre-incubated RAOSMC. Cell viability was detected using the MTT assay. * $P < 0.05$, compared with non-stimulation control; # $P < 0.05$ compared with the 10 ng/ml PDGF-bb stimulated control. (B) The effect of EGCG preincubation on PDGF-bb induced DNA synthesis in RAOSMC. DNA synthesis was detected using the BrdU incorporation assay. * $P < 0.05$, compared with non-stimulation control; # $P < 0.05$ compared with10 ng/ml PDGF-bb stimulated control.

(C)

EGCG		Cell cycle distribution (%)		
	μM	G0/G1	S	G2/M
Serum free		92.83	1.31	5.86
10 ng/ml PDGF-bb	0	78.24	13.27	8.49
	10	81.24	12.93	5.83
	20	89.27	4.38	6.35
	50	89.81	3.73	6.47
	80	89.86	3.71	6.43
	100	88.70	5.23	6.07

Figure 2-1. (continued) (C) EGCG preincubation with PDGF-bb stimulated cell cycle distribution in RAOSMC. Cell cycle distribution was determined by propidium iodide (PI) labeling followed by flow cytometry. The percentages of cells in the G0/G1, S, and G2/M phases were calculated using Modifit computer software and represented within the histograms.

B. Inhibitory effect of proliferation by PDGF-bb stimulation with EGCG on RAOSMC

To investigate proliferation by PDGF-bb stimulation with EGCG on RAOSMC, synchronized cells were for 24 h incubated with increasing EGCG and 10ng/ml PDGF-bb. Treatment with EGCG and PDGF-bb were significantly inhibited the proliferation of RAOSMC by PDGF-bb stimulation (Fig. 2-2A). Therefore DNA synthesis was observed to have similar inhibition with cell viability (Fig. 2-2B). Treatment with EGCG and PGDF-bb resulted in a reduction in BrdU incorporation into RAOSMC at concentrations of 10 μM and more inhibitory effects were observed than RAOSMC preincubated with EGCG. Complete inhibition of proliferation was observed at a concentration of 50 μM. Cells were initially synchronized with serum-free medium for 24 h and incubated with PDGF-bb and increased concentration of EGCG for 24 h. EGCG induced a significant accumulation of cells in the G0/G1 phase of the cell cycle at up 10 μM. These results suggest that the observed cell growth inhibitory effects of EGCG in RAOSMC were due to G0/G1 arrest by EGCG interruption of PDGF-bb stimulation in cell cycle progression.

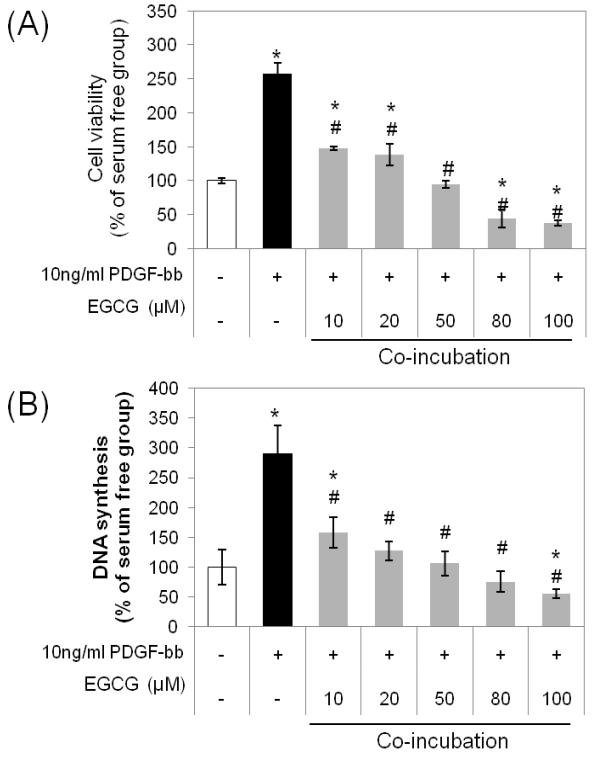

Figure 2-2. Anti-proliferative activity and cell cycle arrest activity by PDGF-bb with EGCG on RAOSMC. After 24 h of starvation with serum free DMEM, cells were treated with 10ng/ml PDGF-bb and increasing concentrations (10 – 80 μM) of EGCG for 24 h (A) The effect of EGCG growth inhibition on PDGF-bb stimulation in RAOSMC. Cell viability was detected using the MTT assay. (B) The effect of EGCG on PDGF-bb induced DNA synthesis in RAOSMC. DNA synthesis was detected using the BrdU incorporation assay. *P < 0.05, compared with non-stimulation control; # P < 0.05 compared with10 ng/ml PDGF-bb stimulated control.

(C)

	EGCG	Cell cycle distribution (%)		
	μM	G0/G1	S	G2/M
	Serum free	92.83	1.31	5.86
10ng/ml PDGF-bb	0	78.24	13.27	8.49
	10	87.05	8.18	4.76
	20	86.08	6.21	7.70
	50	88.52	2.95	8.54
	80	88.88	2.94	8.18
	100	86.83	4.59	8.57

Figure 2-2. (continued) (C) The effect of EGCG on PDGF-bb stimulated cell cycle distribution in RAOSMC. Cell cycle distribution was determined by propidium iodide (PI) labeling followed by flow cytometry. The percentages of cells in the G0/G1, S, and G2/M phases were calculated using Modifit computer software and represented within the histograms.

C. Prevent effect of active MMP-2/9 production by EGCG on PDGF-bb stimulated RAOSMC

MMP-2 and MMP-9 were detected in the conditioned media from cultured RAOSMC for 24 h with EGCG and PDGF-bb by gelatin zymography assay. After stimulation with PDGF-bb, RAOSMC showed more pro-MMP conversion into the intermediated and active form of MMP-2 and increased the MMP-9 release. As shown in Fig. 2-3, EGCG pretreated RAOSMC significantly reduced the PDGF-bb-induced release of MMP-2 activation and MMP-9. Therefore, the stimulatory effect of PDGF-bb also caused a reduction in MMP-2/9 release in a concentration–dependent manner by treatment of RAOSMC with EGCG. The inhibitory effect of MMP release was dose-dependent on EGCG. The active form of MMP-2 was not detected at up 20 μM of EGCG.

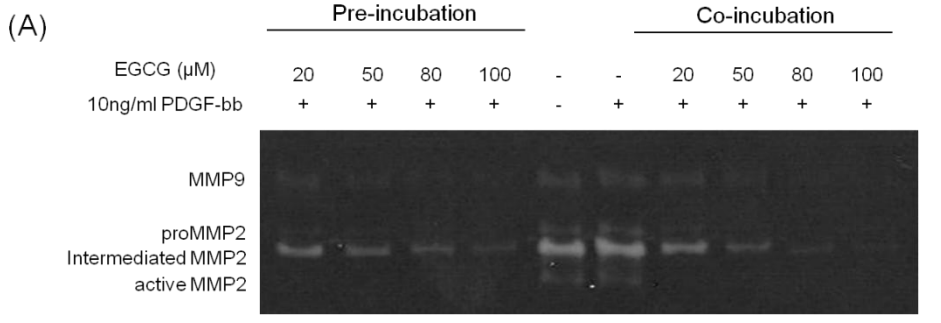

Figure 2-3. (A) Inhibitory effect of EGCG on PDGF-bb induced MMP secretion in RAOSMC. Gelatin catalytic activity was analyzed by gelatin zymography using conditioned medium.

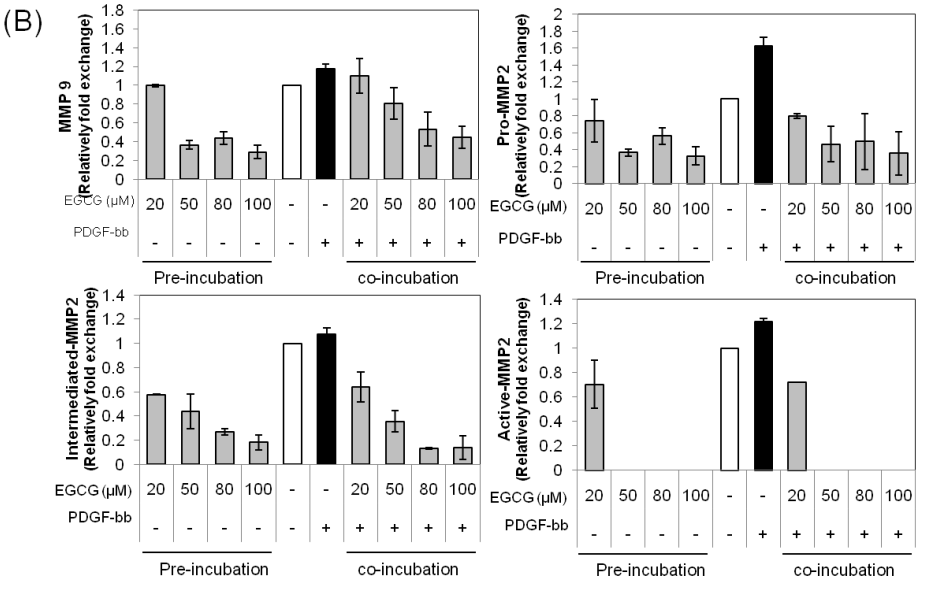

Figure 2-3. (Continued) (B) Band intensity was normalized by densitometry. PDGF-bb induced the secretion of MMP-9 and activity MMP-2. However, both pre-incubated and co-incubated EGCG inhibited secretion of PDGF-bb-induced MMP-9 and activity MMP-2.

D. Inhibitory effect of PDGF-bb stimulated signal transduction pathway in EGCG preincubated RAOSMC

To define to the effects of EGCG pretreatment on signaling pathways of PDGF-stimulated mitogenesis, EGCG was incubated with serum free media for 24 h on RAOSMC. For PDGF-bb stimulation, cells were washed using PBS to removed EGCG, incubated for the desired time, and examined for levels of various proteins by Western blot analysis. Addition of 10 ng/ml PDGF-bb to serum-starved RAOSMCs led to complete PDGFR-β phosphorylation which peaked within 10 min and then decreased to nearly baseline levels at 240 min. However, pre-treated EGCG suppressed PDGFR-β phosphorylation by PDGF-bb and sustained only baseline level. (Fig. 2-4A) The phosphorylation of MEK1/2 and p42-44MAPK, a downstream protein of PDGF-induced signaling, were significantly increased between 10 and 30 min, and declined over the following 240 min. However, pretreated EGCG inhibited MEK1/2 and p42-44MAPK phosphorylation in a time-dependent manner, similarly to PDGFR-β phosphorylation. (Fig. 2-4B) Therefore, other intracellular signal pathways, phosphorylation of Akt and p38 MAPK, was activated by PDGF-bb stimulation. (Fig. 2-4C) These results suggest that EGCG can indirectly inhibit the binding of PDGF-bb with PDGFR-β.

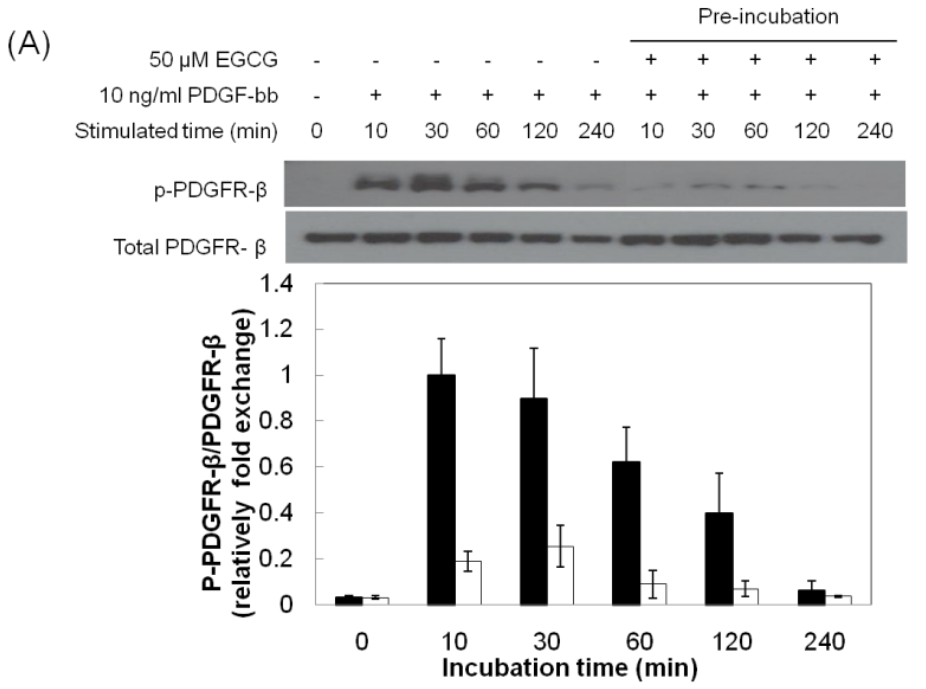

Figure 2-4. Modulation of PDGF-bb stimulatory signal pathways on EGCG preincubated RAOSMC. RAOSMC preincubated with EGCG were stimulated with 10 ng/ml PDGF-bb for the desired time (10 m, 30 m, 1 h, 2 h, and 4 h, respectively), lysed, and lysates were immunoblotted with antibodies. After densitometric quantification, data were each expressed as the mean ± SD from three independent experiments. The black bars indicate expression by PDGF-bb stimulation. The white bars indicate expression by PDGF-bb stimulation on EGCG-pretreated RAOSMC. (A) The expression of phosphor PDGFR-β in a time-dependent manner. The band intensity was normalized to PDGFR-β expression.

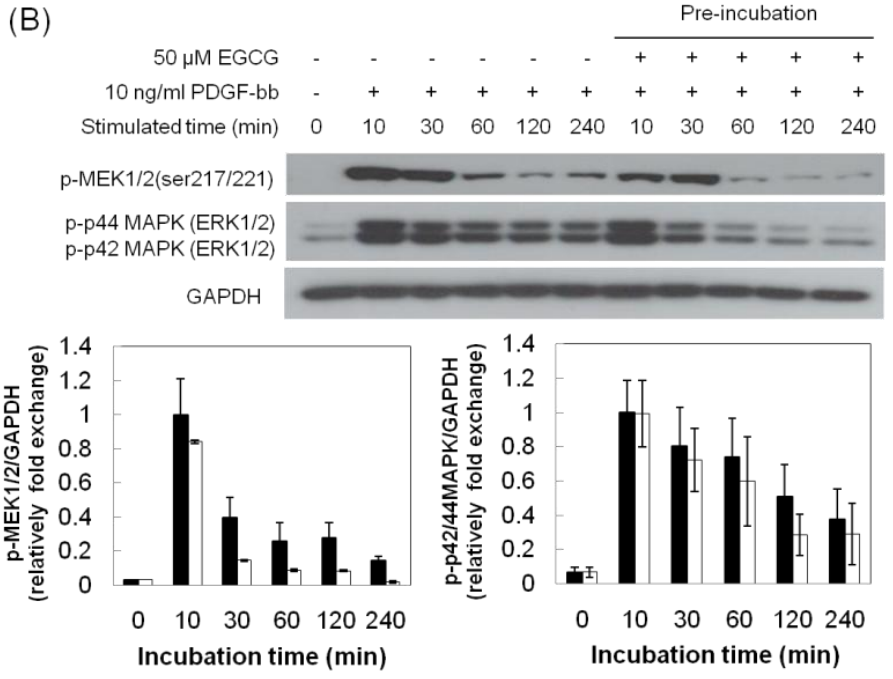

Figure 2-4. (continued) (B) The expression of phosphor MEK1/2 and phosphor-p42/44MAPK in a time-dependent manner. The band intensity was normalized to GAPDH expression.

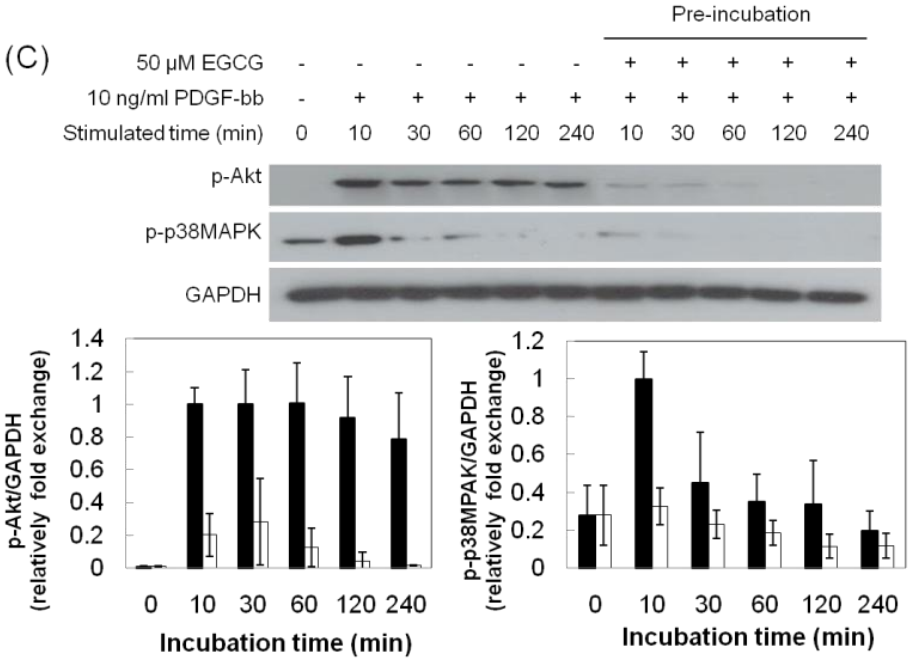

Figure 2-4. (continued) (C) The expression of phosphor Akt and phosphor p38 MAPK on time dependent manner. The band intensity was normalized to GAPDH expression.

E. Inhibitory effect of signal transduction pathway on RAOSMC by PDGF-bb stimulation with EGCG

To characterize the signaling pathways by direct interaction between EGCG and PDGF-bb, serum-starved RAOSMC was incubated with EGCG and PDGF-bb in a time-dependent manner. PDGFR-β phosphorylation was completely suppressed and inactivated on PDGF-bb induced RAOSMC by EGCG as compared with the PDGF-stimulated samples that were processed on the same blot (Fig. 2-5A). Therefore, MEK1/2 and p42/44 MAPK phosphorylation was suppressed and sustained at baseline levels by soluble EGCG (Fig. 2-5B). The phosphorylation of Akt and p38MAPK was also suppressed by inhibition of PDGF-bb signaling by EGCG. These results reveal that EGCG can direct interrupt PDGF-bb stimulation by PDGFR-β phosphorylation.

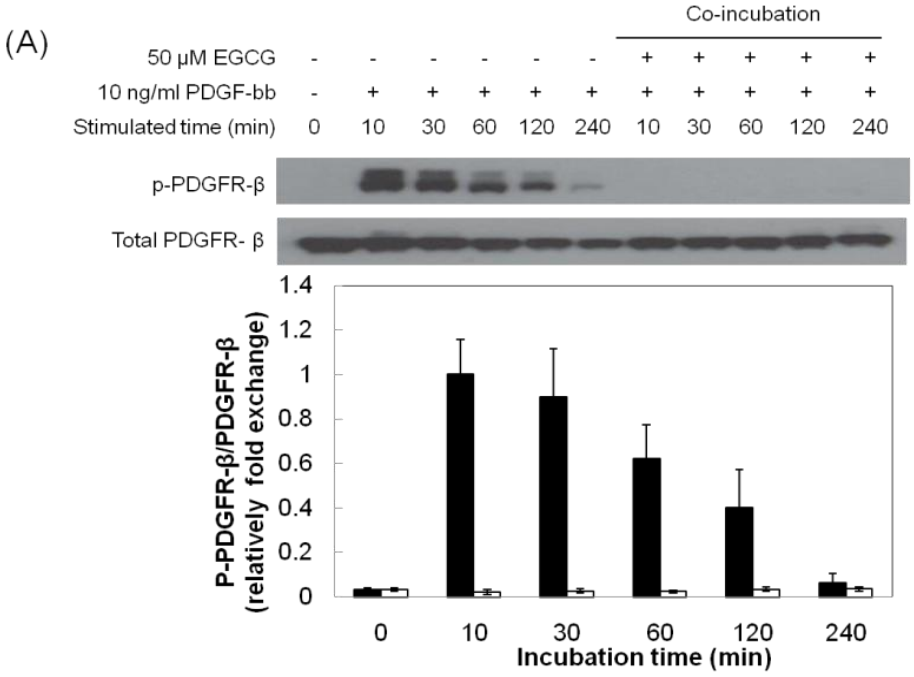

Figure 2-5. The effect of EGCG on modulation of PDGF-bb stimulatory signal pathways in RAOSMC. Serum-starved RAOSMC were stimulated with 10 ng/ml PDGF-bb and 50 μM EGCG for the desired time (10 m, 30 m, 1 h, 2 h, and 4 h, respectively), lysed, and lysates were immunoblotted with antibodies. After densitometric quantification using the imageJ program, data were each expressed as the mean ± SD from three independent experiments. The black bar indicates expression by PDGF-bb stimulation. The white bar indicates expression by PDGF-bb stimulation with EGCG. (A) The expression of phosphor PDGFR-β in a time-dependent manner. The band intensity was normalized to PDGFR-β expression.

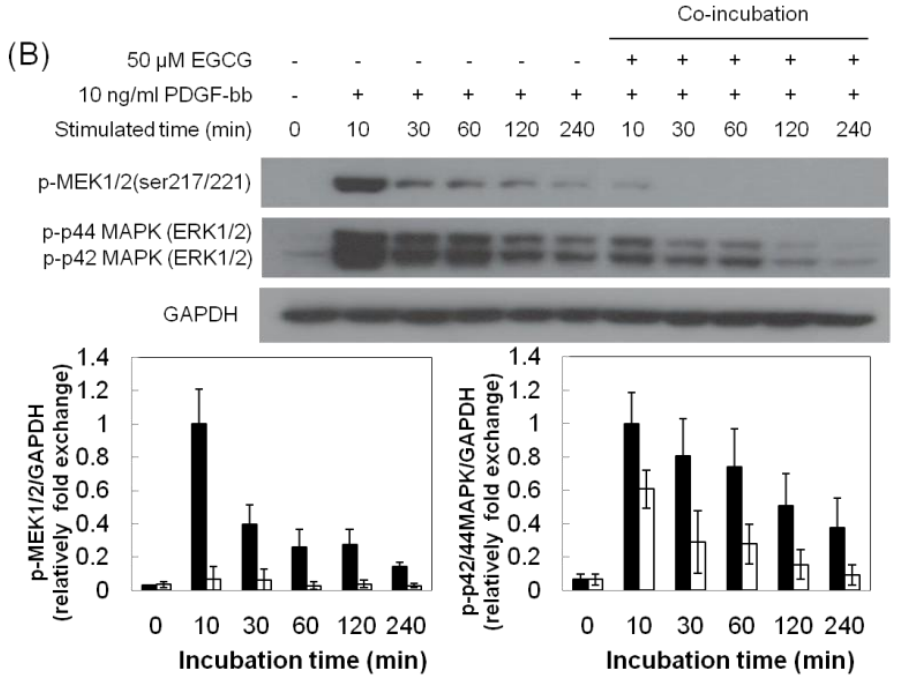

Figure 2-5. (continued) (B) The expression of phosphor MEK1/2 and phosphor p42/44MAPK in a time-dependent manner. The band intensity was normalized to GAPDH expression.

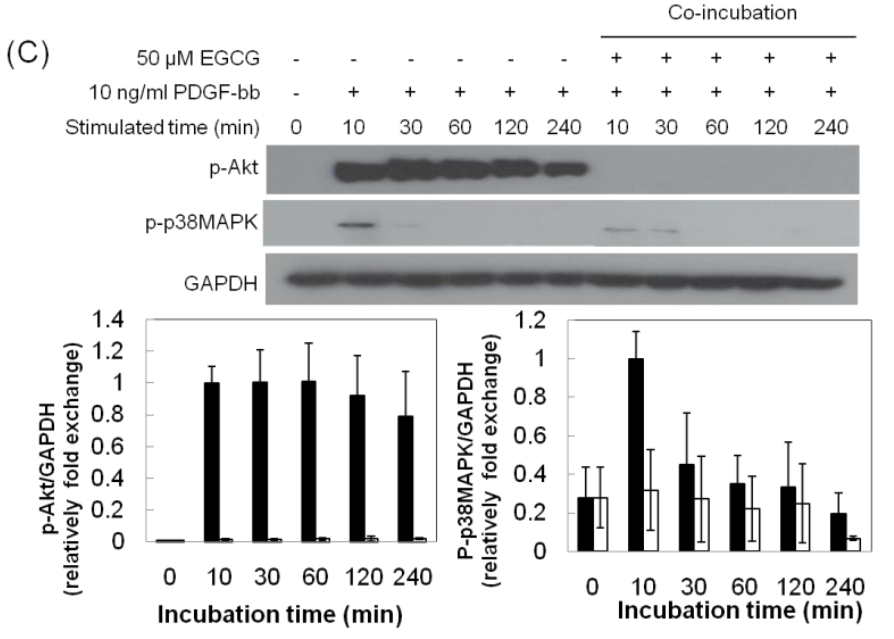

Figure 2-5. (continued) (C) The expression of phosphor Akt and phosphor p38 MAPK in a time-dependent manner. The band intensity was normalized to GAPDH expression.

4. Discussion

PDGF-bb is major stimulator of VSMC dedifferentiation and is known to play a central role in the pathogenesis of various vascular disorders. Signal transduction pathways involve the activation of mitogen-activated protein kinases (MAPKs) on PDGF-induced responses. MAPK is a family of serine/threonine protein kinases with 3 subfamilies named c-jun-N-terminal kinase 1/2 (JNK 1/2), ERK 1/2, and p38 MAPK. PDGF stimulated rapid and significant activation of Akt, ERK 1/2, and p38 MAPK in cultured VSMC. MAPKs are proposed to play a major role in the activation of various transcription factors [16,17]. PDGF-bb binds with PDGFR-β and triggers receptor dimerization and autophosphorylation at tyrosine residues that activate the kinase and serve as recruitment sites for SH_2 domain-containing proteins. Within minutes, many signaling modules are engaged, including Ras, Src, phosphoinositide 3'-kinase (PI3K), SHP_2 and phospholipase Cγ(PLCγ) [18-20]. Downstream signals then activate PI3-K/PKB (Akt) and two MAPK pathways [21]. VSMC dedifferentiation is determined by activation of Akt pathway, p42/44 MAPK, and p38MAPK pathways. Ultimately, this results in VSMC dedifferentiation in the recruitment and activation of specific signaling pathway that may mediate the migration and proliferation of VSMCs in response to injury such as the development of atherosclerosis and hypertension. Several studies have revealed that PDGFR targeting using synthetic tyrosine kinase inhibitors and antisense treatment have been described to reduce neointima

formation in injured arteries [22,23].

EGCG has been shown to have protective effects on the cardiovascular system, including anti-atherosclerotic, anti-hypercholesterolemic, and anti-restenosis effects [24-26]. Also, several studies have stated that EGCG inhibited proliferation, migration, and invasion of barrier by inhibition via intracellular signaling transduction pathway signals on VSMC stimulated with growth factor, such as angiotensin II [27,28] and basic fibroblast growth factor (bFGF)[29]. A previous study showed that EGCG induced apoptosis of VSMCs in a p53 and NF-κB-dependent manner [30,31].

Our results observed that RAOSMC stimulation by PDGF-bb induced proliferation and cell cycle progression through intracellular pathways; p42/44 MAPK, p38MAPK and Akt cascade, in addition to the activation of PDGFR-β. However, PDGF-bb was not induced to proliferation and mitogenesis on RAOSMC pre-incubated with EGCG (Fig. 2-1). Also, preincubated EGCG inhibited the secretion of MMP-9 and conversion from pro MMP-2 to active MMP-2. (Fig. 2-3) These results suggest that EGCG may mediate the inhibition of PDGF-bb directly binding with PDGFR-β on the ROAMS membrane and thus deactivate the PDGF signal pathway related to mitogenesis (Fig 2-4). Some studies reported that EGCG is hijacked by the laminin receptor (LamR), a lipid raft protein, and alters membrane domain composition, also preventing epidermal growth factor (EGF) from binding to its receptor (EGFR), as well as the dimerization of EGFR and the relocation of phosphorylated EGFR to lipid

rafts [32,33]. Also, EGCG has been shown to incorporate itself to the plasma membrane and to lead to reversible binding of PDGF-bb to a non-receptor target site, reducing PDGF binding to its receptors [34]. Thus, EGCG distributes action through a surface-membrane linked mechanism [35].

In this study, we could also demonstrate experiments on the direct interaction between soluble EGCG and PDGF-bb. As shown in Fig. 2, low concentration of EGCG (10 μM) induces anti-proliferation and cell cycle arrest, and cell stimulation occrred in the presence of EGCG. This effect is accompanied by the fact that EGCG inhibits PDGF-induced mitogenesis by disturbing PDGFR-β phosphorylation (Fig. 2-5). Also, the inhibitory effect of EGCG was mediated by the blockagage of PDGFR-β phsophorylation early on in the experiment. Thus, EGCG may already have interacted with PDGF-bb in media and inhibited VSMC dedifferentiation by blocking the early signal transduction pathway. Another group showed that EGCG is able to interact with various biomolecules, especially proliferation-related proteins by various cell line experiments [36-41]. Therefore, recent studies have revealed that EGCG binds with high affinity to residues located in the serum albumin under physiological conditions by physical analysis [42,43]. Based on our findings, we suggest that EGCG inhibited RAOSMC dedifferentiation by interrupting the PDGF-bb signal, probably by blocking PDGF-bb binding and PDGFR-β phosphorylation, and an important downstream event PDGFR-β, the activation of p42/44 MAPK, p38MAPK, and Akt.

5. Conclusion

In this study we investigated the effect of EGCG on signal transduction pathways induced by PDGF-bb. Both soluble and preincubated EGCG significantly inhibited PDGF-bb-induced proliferation, cell cycle progression of G0/G1 phase, and MMP-2/9 secretion on RAOSMC. Also, EGCG also blocked PDGF receptor-β (PDGFR-β) phosphorylation on PDGF-bb stimulated ROAMSC under pre-treatment with cell as well as soluble co-treatment with PDGF-bb. The downstream signal transduction pathways of PDGF-Rβ, including p42/44 MAPK, p38, and Akt phosphorylation, were also inhibited by EGCG in the similar pattern compared with PDGF-Rβ phosphorylation. Based on our findings, we suggest that EGCG inhibited RAOSMC dedifferentiation by interruption of PDGF-bb signal, probably by blocking of PDGF-bb bind and PDGFR-β phosphorylation, and of an important downstream event PDGFR-β, the activation of p42/44 MAPK, p38MAPK, and Akt. Therefore, EGCG may the potential inhibitors of targeting the PDGFR and be used for the prevention and treatment of vascular diseases.

6. References

1. Willis AI, Pierre-Paul D, Sumpio BE, Gahtan V. Vascular Smooth Muscle Cell Migration: Current Research and Clinical Implications Vasc Endovascular Surg 2004; 38; 11-23.
2. Davies MG, Hagen PO. Pathobiology of intimal hyperplasia. Br J Surg 1994; 81:1254-69.
3. Coats WD, Faxon DP. The role of the extracellular matrix in arterial remodelling. Semin Intervent Cardiol 1997; 2:167-76.
4. Schwartz SM. Smooth muscle migration in atherosclerosis and restenosis. J Clin Invest 1997; 99:2814-7.
5. Snow AD, Bolender RP, Wight TN, Clowes AW. Heparin modulates the composition of the extracellular matrix domain surrounding arterial smooth muscle cells. Am J Pathol 1990;137:313–30.
6. Kraiss LW, Kirkman TR, Kohler TR, Zierler B, Clowes AW. Shear stress regulates smooth muscle proliferation and neointimal thickening in porous polytetrafluoroethylene grafts. Arterioscler Thromb 1991;11:1844–52.
7. Heldin CH, Westermark B. Mechanism of action and in vivo role of platelet-derived growth factor. Physiol Rev 1999;79:1283–316.
8. El Bedoui J, Oak MH, Anglard P, Schini-Kerth VB. Catechins prevent vascular smooth muscle cell invasion by inhibiting MT1-MMP activity and MMP-2 expression. Cardiovasc Res 2005;67(2):317-25.
9. Risinger GM Jr, Updike DL, Bullen EC, Tomasek JJ, Howard EW. TGF-

beta suppresses the upregulation of MMP-2 by vascular smooth muscle cells in response to PDGF-BB. Am J Physiol Cell Physiol 2010; 298(1):C191-201.

10. Zhan Y, Kim S, Izumi Y, Izumiya Y, Nakao T, Miyazaki H, Iwao H. Role of JNK, p38, and ERK in platelet-derived growth factor-induced vascular proliferation, migration, and gene expression. Arterioscler Thromb Vasc Biol 2003;23(5):795-801.
11. Yamaguchi H, Igarashi M, Hirata A, Tsuchiya H, Susa S, Tominaga M, et al. Characterization of platelet-derived growth factor-induced p38 mitogen-activated protein kinase activation in vascular smooth muscle cells. Eur J Clin Invest 2001;31(8):672-80.
12. Cheng XW, Kuzuya M, Nakamura K, Liu Z, Di Q, Hasegawa J, et al. Mechanisms of the inhibitory effect of epigallocatechin-3-gallate on cultured human vascular smooth muscle cell invasion. Arterioscler. Thromb Vasc.Biol 2005;25;1864-70.
13. Kim CH, Moon SK. Epigallocatechin-3-gallate causes the p21/WAF1-mediated G1-phase arrest of cell cycle and inhibits matrix metalloproteinase-9 expression in TNF-a-induced vascular smooth muscle cells. Arch Biochem Biophys 2005;435;264–72.
14. Chen D, Milacic V, Chen MS, Wan SB, Lam WH, Huo C, et al. Tea polyphenols, their biological effects and potential molecular targets. Histol Histopathol 2008;23(4):487-96.

15. Maeda K, Kuzuya M, Cheng XW, Asai T, Kanda S, Tamaya-Mori N, et al. Green tea catechins inhibit the cultured smooth muscle cell invasion through the basement barrier. Atherosclerosis 2003;166(1):23-30.
16. Romano F, Chiarenza C, Palombi F, Filippini A, Padula F, Ziparo E, et al. Platelet-derived growth factor-BB-induced hypertrophy of peritubular smooth muscle cells is mediated by activation of p38 MAP-kinase and of Rho-kinase. J Cell Physiol 2006;207(1):123-31.
17. Reusch HP, Zimmermann S, Schaefer M, Paul M, Moelling K. Regulation of Raf by Akt controls growth and differentiation in vascular smooth muscle cells. J Biol Chem 2001;276(36):33630-7.
18. Heldin CH, Westermark B. Mechanism of action and in vivo role of platelet-derived growth factor. Physiol Rev 1999;79(4):1283-316.
19. Fredriksson L, Li H, Eriksson U. The PDGF family: four gene products form five dimeric isoforms. Cytokine Growth Factor Rev 2004;15(4):197-204.
20. Pawson T. Protein modules and signaling networks. Nature 1995;373(6515):573-80.
21. Hayashi K, Takahashi M, Kimura K, Nishida W, Saga H, Sobue K. Changes in the balance of phosphoinositide 3-kinase/protein kinase B (Akt) and the mitogen-activated protein kinases (ERK/p38MAPK) determine a phenotype of visceral and vascular smooth muscle cells. J Cell Biol 1999;145(4):727-40.

22. Bilder G, Wentz T, Leadley R, Amin D, Byan L, O'Conner B, et al. Restenosis following angioplasty in the swine coronary artery is inhibited by an orally active PDGF-receptor tyrosine kinase inhibitor, RPR101511A. Circulation 1999;99:3292–9.
23. Noiseux N, Boucher CH, Cartier R, Sirois MG. Bolus endovascular PDGFR-beta antisense treatment suppressed intimal hyperplasia in a rat carotid injury model. Circulation 2000;102:1330–6.
24. Chyu KY, Babbidge SM, Zhao X, Dandillaya R, Rietveld AG, Yano J, et al. Differential effects of green tea-derived catechin on developing versus established atherosclerosis in apolipoprotein E-null mice. Circulation 2004;109(20):2448-53.
25. Maron DJ, Lu GP, Cai NS, Wu ZG, Li YH, Chen H, et al. Cholesterol-lowering effect of a theaflavin-enriched green tea extract. A randomized controlled trial. Arch Intern Med 2003;163(12):1448-53.
26. Kim DW, Park YS, Kim YG, Piao H, Kwon JS, Hwang KK, et al. Local delivery of green tea catechins inhibits neointimal formation in the rat carotid artery injury model. Heart Vessels 2004;19(5):242-7.
27. Zheng Y, Song HJ, Kim CH, Kim HS, Kim EG, Sachinidis A, et al. Inhibitory effect of epigallocatechin 3-O-gallate on vascular smooth muscle cell hypertrophy induced by angiotensin II. J Cardiovasc Pharmacol 2004;43(2):200-8.
28. Won SM, Park YH, Kim HJ, Park KM, Lee WJ. Catechins inhibit

angiotensin II-induced vascular smooth muscle cell proliferation via mitogen-activated protein kinase pathway. Exp Mol Med 2006;38(5):525-34.

29. Hwang KC, Lee KH, Jang Y, Yun YP, Chung KH. Epigallocatechin-3-gallate inhibits basic fibroblast growth factor-induced intracellular signaling transduction pathway in rat aortic smooth muscle cells. J Cardiovasc Pharmacol 2002;39(2):271-7.
30. Hofmann CS, Sonenshein GE. Green tea polyphenol epigallocatechin-3 gallate induces apoptosis of proliferating vascular smooth muscle cells via activation of p53. FASEB J 2003;17(6):702-4.
31. Han DW, Lim HR, Baek HS, Lee MH, Lee SJ, Hyon SH, et al. Inhibitory effects of epigallocatechin-3-O-gallate on serum-stimulated rat aortic smooth muscle cells via nuclear factor-kappaB down-modulation. Biochem Biophys Res Commun 2006;345(1):148-55.
32. Patra SK, Rizzi F, Silva A, Rugina DO, Bettuzzi S. Molecular targets of (-)-epigallocatechin-3-gallate (EGCG): specificity and interaction with membrane lipid rafts. J Physiol Pharmacol 2008;59 Suppl 9:217-35.
33. Rodriguez SK, Guo W, Liu L, Band MA, Paulson EK, Meydani M. Green tea catechin, epigallocatechin-3-gallate, inhibits vascular endothelial growth factor angiogenic signaling by disrupting the formation of a receptor complex. Int J Cancer 2006;118(7):1635-44.
34. Weber AA, Neuhaus T, Skach RA, Hescheler J, Ahn HY, Schrör K, et al.

Mechanisms of the inhibitory effects of epigallocatechin-3 gallate on platelet-derived growth factor-BB-induced cell signaling and mitogenesis. FASEB J 2004 ;18(1):128-30.

35. Liang YC, Chen YC, Lin YL, Lin-Shiau SY, Ho CT, Lin JK. Suppression of extracellular signals and cell proliferation by the black tea polyphenol, theaflavin-3,3′-digallate. Carcinogenesis 1999;20 (4):733–6.
36. Zheng X, Chen A, Hoshi T, Anzai J, Li G. Electrochemical studies of (-)-epigallocatechin gallate and its interaction with DNA. Anal Bioanal Chem 2006;386(6):1913-9.
37. Kitano K, Nam KY, Kimura S, Fujiki H, Imanishi Y. Sealing effects of (-)-epigallocatechin gallate on protein kinase C and protein phosphatase 2A. Biophys Chem 1997;65:157–64.
38. Wang ZY, Das M, Bickers DR, Mukhtar H. Interaction of epicatechins derived from green tea with rat hepatic cytochrome P-450. Drug Metab. Dispos 1988;16:98–103
39. Sazuka M, Itoi T, Suzuki Y, Odani S, Koide T, Isemura M. Evidence for the interaction between (-)-epigallocatechin gallate and human plasma proteins fibronectin, fibrinogen, and histidine-rich glycoprotein. Biosci Biotechnol Biochem 1996;60:1317–9.
40. Sazuka M, Isemura M, Isemura S. Interaction between the carboxyl-terminal heparin-binding domain of fibronectin and (-)-epigallocatechin gallate. Biosci Biotechnol iochem 1998;62:1031–2.

41. Nam S, Smith DM, Dou QP. Ester bond-containing tea polyphenols potently inhibit proteasome activity in vitro and in vivo. J Biol Chem 2001;276:13322–30.
42. Maiti TK, Ghosh KS, Dasgupta S. Interaction of (-)-epigallocatechin-3-gallate with human serum albumin: fluorescence, fourier transform infrared, circular dichroism, and docking studies. Proteins 2006;64(2):355-62.
43. Nozaki A, Hori M, Kimura T, Ito H, Hatano T. Interaction of polyphenols with proteins: binding of (-)-epigallocatechin gallate to serum albumin, estimated by induced circular dichroism. Chem Pharm Bull (Tokyo). 2009;57(2):224-8.

III. RESVERATROL REGULATES PHENOTYPE MODULATION BY REGULATION OF AKT AND mTOR PHOSPHORYLATION ON PLATELET DERIVED GROWTH FACTOR –BB INDUCED RAT AORTA SMOOTH MUSCLE CELLS

1. Introduction

Dedifferented VSMCs of the media layers are phenotypicall modulated from contractile state to the active synthetic state and induce proliferation and migration of VSMC from the media to the intima and extracellular matrix (ECM) protein deposition [1~3]. Differentiated VSMC in normal vessel have contractile phenotype and spindle elongated morphology, and decrease cell size, while dedifferentiated VSMC in injured vessel have synthetic phenotype, hypertrophic appearance, hill and valley growth, and increased cell size. In addition to these morphological and functional alterations, change of VSMC from contractile to synthetic phenotype is controlled by SMC-specific molecular markers such as caldesmon, calponin, a-trypomyosin, smooth muscle myosin heavy chain, SM22α, smooth muscle alpha actin (αSMA) etc [4~6].

Platelet-derived growth factor-bb (PDGF-bb) is one of the most potent mitogens and chemoattractants for VSMC. PDGF-bb binds to the PDGR receptor (PDGFR)-β and subsequently activates several intracellular signaling cascades, including the extracellular signal–regulated kinase (ERK), p38 mitogen–activated protein kinase (p38 MAPK) pathways, and phosphatidylinositol 3-kinase-Akt (PI3K-Akt), and stimulates VSMC dedifferentiation [7,8]. Akt is the

major signal in growth factor-mediated transcription and promotes cell survival by inhibiting apoptosis. Beside, Akt pathway is the key trigger of mTOR signaling and Akt-mediaed phosphorylation is directly related to mTOR activation. The mTOR is implicated in cardiovascular diseases and more particularly in cardiac hypertrophy [9,10].

Resveratrol (3,4',5 trihydroxystilbene), a naturally-occurring molecule known as a phytoalexin, is polyphonic compound found in grape and red wine. Also, resveratrol is known to possess antioxidant, anti-inflammatory, anti-thrombotic and anti-proliferative effect. Additionally, various studies have shown that resveratrol inhibits the oxidation of low-density lipoprotein, early progression of atherosclerotic lesions and protects cardiomyocytes against ischaemia–reperfusion injury [11~13].

In this study, we investigate the effects of EGCG on proliferation, cell cycle and the intracellular signal transduction pathway on PDGF-bb induced rat aortic vascular smooth muscle cell (RAOSMC) and demonstrate the inhibitory mechanism on phenotype modulation of PDGF-bb stimulated RAOSMC.

2. Materials & Methods

A. Cell Culture

Primary cultured rat aortic smooth muscle cells (RAOSMC, biobud, Seoul, Korea) were routinely maintained in Dulbecco's modified Eagles medium (Gibco, Carlsbad, CA, USA) supplemented with 10% fetal bovine serum (Sigma, St. Louis, MO, USA) and a 1% antibiotic-antimycotic solution containing 10,000 units penicillin, 10 mg streptomycin, and 25 μg/ml amphotericin B (Sigma) at 37℃ in a humidified atmosphere of 5% CO_2. For experiment, cells were used between passage 5 and 9.

B. Cell Stimulation by PDGF-bb

RAOSMC were grown to 80~90% confluence and synchronized in serum free DMEM medium for 48 h before experiments. Trans-resveratrol (Sigma) was dissolved in 50% DMSO (Sigma) for a stock solution of 100 mM and then diluted to desired concentrations with media prior to cell treatment. Quiescent cells were incubated with or without PDGF-bb (10 ng/ml) and resveratrol for designed time.

C. Cell Proliferation and DNA synthesis.

Cell proliferation was determined by MTT assay [reduction of 3-(4,5-dimethylthiazol-2-yl)-2,5-diphenyltetrazolium bromide to a purple formazan

product, Sigma] and a 5-bromo-2'-deoxyuridine (BrdU) incorporation assay (Roche applied science, Basel, Switzerland).

For the MTT assay, the cells were incubated with 0.5 mg/ml of MTT in the last 4 h of the culture period tested at 37 ℃ in the dark. The media were decanted and the produced formazan salts were dissolved with dimethylsulphoxide, and absorbance was determined at 570 nm by an automatic microplate reader (Spectra Max 340, Molecular Devices, Inc., Sunnyvale, CA, USA).

For BrdU incorporation assay, BrdU-labeling solution was added to the cells, which were then reincubated the cell for 2 h at 37 ℃. Labeling medium was then removed and the cells were incubated with fixation solution for 30 min at room temperature. After fixation of the cells, anti-BrdU-POD working solution was added and the cells were incubated for 90 min at room temperature. Then, the substrate solution was added and absorbance was measured at 370 nm with 492 nm reference wavelength by an automatic microplate reader (Spectra Max 340, Molecular Devices, Inc.).

D. Gelatin zymography

MMP secretion was detected in the conditioned medium of cultured RAOSMC with various concentration of resveratrol. The conditioned media mixed with laemmli-buffer under non-reducing conditions were loaded onto 10% SDS-polyacrylamide gel containing 0.1% gelatin. After electrophoresis, the gels were washed for 20min at room temperature in 2.5 % Triton X-100 and incubated for

overnight at 37℃ with reaction buffer 50 mM Tris base (pH 7.6), 0.2M NaCl, 5mM CaCl2, 0.02% Brij 35). Gels were stained with Coomassie Brillant Blue R-2500(0.1%) and destained in 5% methanol and 7% acetic acid. Gelatinolytic activity was detected as clear band on a blue background. Band density were calculated with imageJ image (National Institutes of Health, Bethesda, MD, USA).

E. Immunofluorescence assay

Cells were grown onto coverslips at 50% confluence, were serum starved for 48 h and then stimulated with or without 10ng/ml PDGF-bb and resveratrol. Stimulated cells were fixed in 10% formalin solution and permeabilized with 0.5% Triton X-100 in phosphate buffer saline (PBS, pH 7.6). Then, cells were blocked with 5% bovine serum albumin (BSA, Sigma) and incubated with anti-smooth muscle actin-α (αSMA, Dako Faramount, Dako North America Inc., CA, USA) and anti-calponin (Santacruz Biotechnology, Santa Cruz, CA, USA). Then cells were incubated with secondary antibody, goat-anti-mouse IgG-conjugated Texas Red (Santacruz). Alexa 488-conjugated rhodamine phalloidin (5 U/ml, Invitrogen) was used to visualize F-actin stress fibers and nucleus was stained by Hoechst 33528. Coverslips were mounted with aqueous mounting medium (Dako Faramount) and images were evaluated using Olympus fluorescence microscope (Melville, NY, USA) with DP-71 digital camera (Olympus).

F. Morphology analysis

For morphology analysis, cell was visualized by staining with Alexa 488-conjugated rhodamine phalloidin (5 U/ml, Invitrogen) and Hoechst 33258 (1 μg/ml in PBS, Sigma). Images were captured on Olympus fluorescence microscope (Melville, NY) with DP-71 digital camera (Olympus, Japan). Cell circularity and area of 100 cells for each group was analyzed by imageJ software (NIH).[15,16] The circularity was measured to determine the morphological distribution between the contractile phenotype and synthetic phenotype of RAOSMC. Circularity represented from 0 to 1, closer to 0 indicated spindles morphology, and closer to 1 indicated circular phenotype.

G. Western blotting

After time-course simulation with PDGF-bb, the cells were washed twice with cold PBS (10 mM, pH 7.4). Ice-cold RIPA lysis buffer (Santa Cruz Biotechnology) was added to the cells for 5 min. The cells were scraped, and the lysate was cleared by centrifugation at 14,000 × g for 20 min at 4℃. The resultant supernatant (total cell lysate) was collected. The protein concentration was determined using a DC Bio-Rad assay kit (Bio-Rad Laboratories). For immunoblot analysis, protein was run on 10~15 % SDS-PAGE and then electrotransfered onto a PVDF membrane. The membrane was blocked with blocking buffer (5% bovine serum albumin and 1% Tween-20 in

20 mM TBS, pH 7.6) for 1 h at room temperature and then probed overnight with phosphor PDGFR-β (pPDGFR-β), PDGFR-β, phosphor MEK1/2 (pMEK1/2), phospho p42/44MAPK (pp42/44MAPK), phosphor Akt (pAkt), phosphor mTOR, and phosphor p38MAPK (pp38MAPK) used in a 1:1,000 dilution from Cell Signaling Technology, respectively. Detection of horseradish peroxidase-conjugated secondary Ab (e.g., anti-rabbit IgG (1:2,000), anti-mouse IgG (1:2,000) from Santacruz Biotechnology Inc.) was accomplished using enhanced chemiluminescence using the ECL Plus detection kit (Amersham Biosciences, Buckinghamshire, England).

H. Statistical Analysis.

All variables were tested in three independent cultures for each experiment. The results are reported as a mean ± SD compared to non-treated controls. Statistical analysis was performed using a one-way (ANOVA), followed by a Tukey HSD test for the multiple comparisons used SPSS software. A P value < 0.05 was considered statistically significant.

3. Results

A. Inhibitory effect of resveratrol on PDGF-bb-induced proliferation in RAOSMC

To assessed the effect of resveratrol on PDGF-bb induced RAOSMC proliferation, serum starved RAOSMC was incubated with 10 ng/ml PDGF-bb and increasing concentration of resveratrol for 48 h. MTT and BrdU assays revealed that incubation of serum-starved RAOSMC with 10 ng/ml PDGF-bb for 48 h increased both DNA synthesis and cell number, compared with the untreated control group. The presence of resveratrol results in significant ($p < 0.05$) dose-dependent decreases in cell growth (Fig. 3-1A). When cells were treated with increasing concentrations of resveratrol, a significant ($p < 0.05$) dose-dependent reduction in cell growth was observed starting at 50 μM. The level of DNA synthesis was also measured as cell proliferation assay. Stimulation of RAOSMC with 10 ng/ml PDGF-bb caused a significant increase in the DNA amount, while resveratrol inhibited significantly the PDGF-bb stimulated DNA synthesis in a concentration-dependent manner (Fig. 3-1B). Also, cell viability and DNA synthesis induced by PDGF-bb stimulation was completely suppressed in more than 100 μM of resveratrol. These results suggest that resveratrol expert potent anti-proliferative activity.

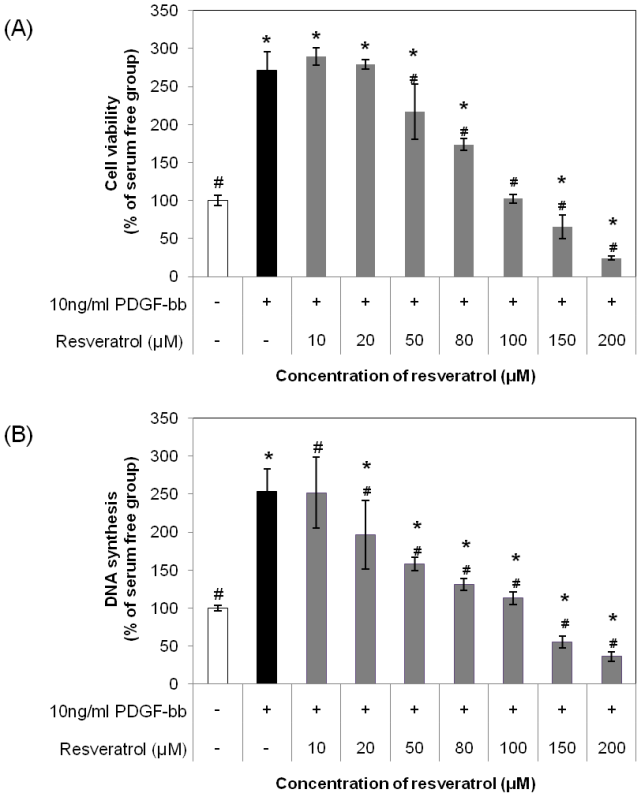

Figure 3-1. Anti-proliferative activity by PDGF-bb with resveratrol on RAOSMC. After 24 h of starvation with serum free DMEM, cells were treated with 10ng/ml PDGF-bb and increasing concentrations (10 – 200 μM) of resveratrol for 48 h (A) The effect of resveratrol growth inhibition on PDGF-bb stimulation in RAOSMC. Cell viability was detected using the MTT assay. (B) The effect of resveratrol on PDGF-bb induced DNA synthesis in resveratrol. DNA synthesis was detected using the BrdU incorporation assay. *P < 0.05, compared with non-stimulation control; # P < 0.05 compared with 10 ng/ml PDGF-bb stimulated control.

B. Inhibitory effect of gelatinolytic activity MMP secretion by resveratrol in RAOSMC

To access of extracellular matrix (ECM) degradation, production of MMP was performed by gelatin zymography assay with the conditioned media from RAOSMC. As shown Fig. 3-2, serum starved RAOSMC was incubated with or without resveratrol and 10 ng/ml PDGF-bb. Presence of resveratrol decreased secretion of MMP-9 and MMP-2 in dose-dependent manner. Therefore, PDGF-bb induced MMP-2 and MMP-9 secretion, while resveratrol reduced concentration dependently the MMP-9 secretion and conversion from pro MMP-2 to active MMP-2. However, the inhibitory effect of gelatinolytic activity was significantly observed in over 150 μM resveratrol.

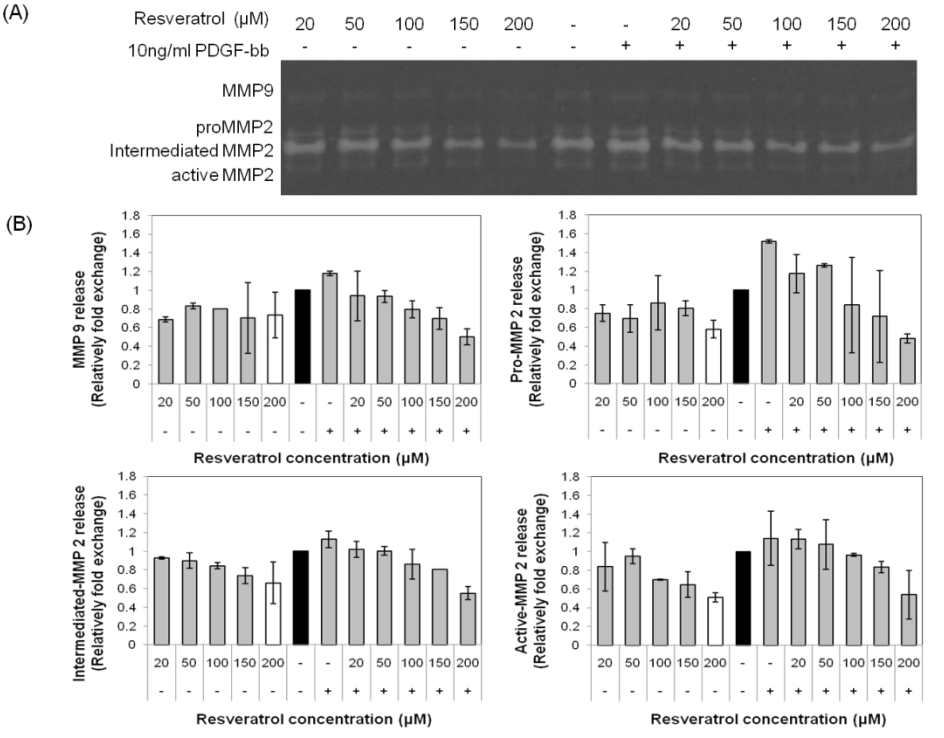

Figure 3-2. The inhibitory effect of resveratrol on PDGF-bb induced MMP secretion in RAOSMC. (A) Gelatin catalytic activity was analyzed by gelatin zymography using conditioned medium. (B) Band intensity was normalized by densitometry. PDGF-bb was induced the secretion of MMP-9 and activity MMP-2. However, both resveratrol inhibited the secretion of PDGF-bb induced MMP-9 and activity MMP-2.

C. Inhibitory effect of resveratrol on PDGF-bb stimulated RAOSMC morphology and phenotype

To define phenotype exchange in PDGF stimulation, we assessed phenotype and morphology using the immunofluorescence and immunocytochemical staining with antibodies against αSMA and calponin on RAOSMC. RAOSMC were grown on glass cover slips, starved serum for 48 h, and stimulated in the presence and absence of PDGF-bb and resveratrol for 24 h, respectively.

RAOSMC exhibited elongation and spindly morphology during prolonged serum deprivation. As shown Fig. 3-3, serum starved RAOSMC revealed aligned arrangement of actin filament with an organized cytoskeleton network, whereas PDGF-bb stimulated RAOSMC modulated disassembled distribution and aggregated around the peri-nuclear region of actin filaments without clear filamentous organization. However, resveratrol treatment maintained spindle-like shape and reorganization of the actin filament by inhibition of PDGF-bb stimulation on RAOSMC as compared with serum starved RAOSMC.

Therefore, cells were present accumulation of contractile related protein, αSMA (Fig. 3-4A) and calponin (Fig. 3-4D) in clear actin filament organization. When cells were stimulated with PDGF-bb, cells were observed morphological changes from spindle to polygonal and revealed of the relatively low level of αSMA (Fig. 3-4B) and calponin (Fig. 3-4E) with disassembled distribution of actin filament in cytosol. However, resveratrol treatment inhibited the morphological change. The actin cytoskeleton maintained into parallel actin

filaments by complex of contractile phenotype related protein, including αSMA (Fig. 3-4C) and calponin (Fig. 3-4F). To determine the morphological distribution, the circularity was measured by imageJ analysis. Compared to serum starved cells, PDGF-bb stimulated cells distributed in greater circularity whereas cell morphology with resveratrol exhibited lower circularity (Fig. 3-5A). The average circularity of PDGF-bb stimulated cell was significantly higher than non-treated cells. However, resveratrol treated cells with PDG-bb were not significantly difference with non-treated cells (Fig. 3-5B). Therefore, PDGF-bb stimulated RAOSMC exhibited greater area, compared with serum starved RAOSMC. Resveratrol inhibited the change of area stimulated by PDGF-bb (Fig. 3-5C).

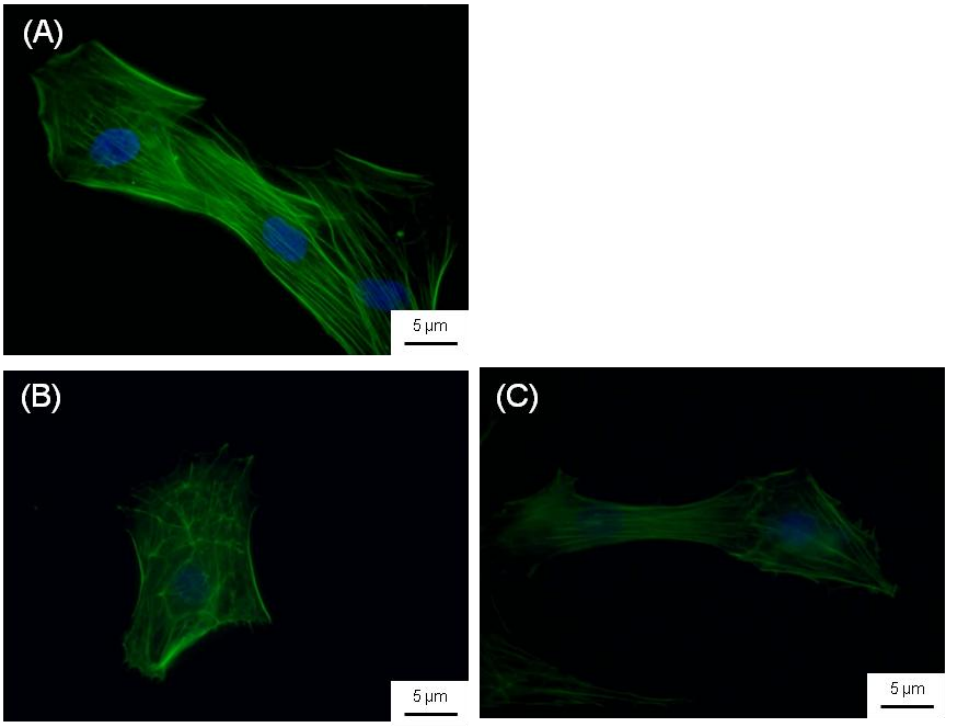

Figure 3-3. Arrange of F-actin filament on RAOSMC with or without 10 ng/ml PDGF-bb and 20 μM resveratrol. (A) Cells in serum free media (B) Cells in 10 ng/ml PDGF-bb (C) Cells in 20 μM resveratrol with 10 ng/ml PDGF-bb. Nuclei stained in blue with Hoechst 33528, F-actin in green with alexa(388)-rhodamine phalloidin. The micrographs (magnification, ×400) shown in this figure are representative of three independent experiments with similar results.

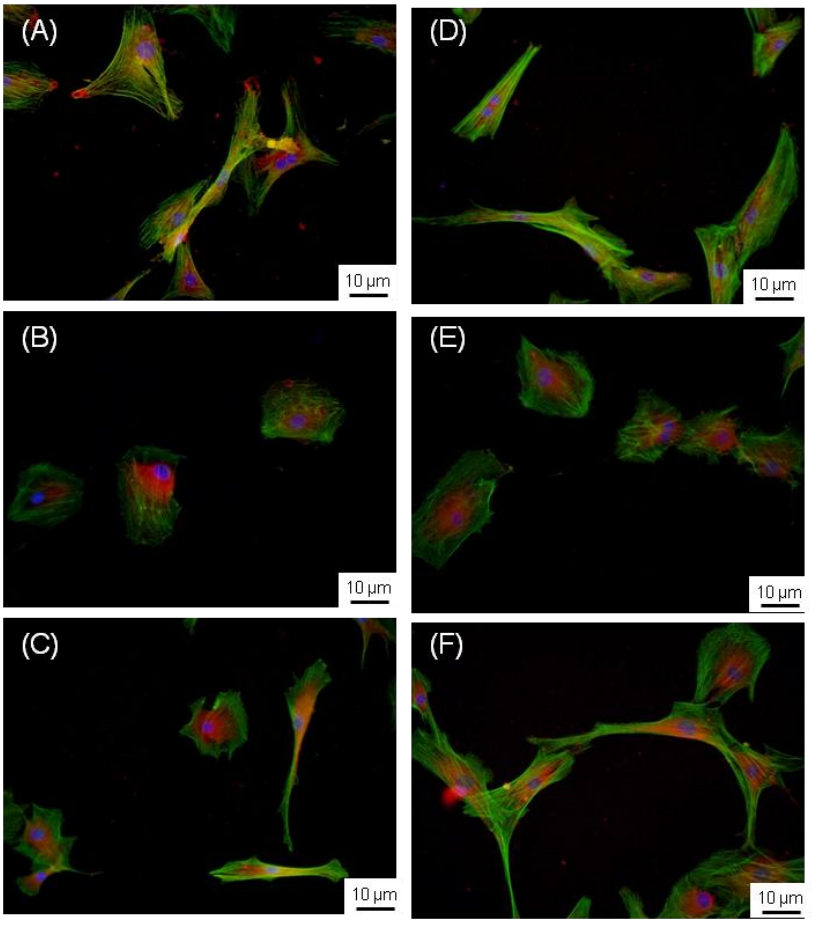

Figure 3-4. Characterization of morphology modulation by resveratrol on PDGF-bb stimulated RAOSMC. Cells were incubated in serum free media (A, D), 10 ng/ml PDGF-bb (B, E), and 20 μM resveratrol with 10 ng/ml PDGF-bb (C, F). Nuclei stained in blue with Hoechst 33528, αSMA(A~C) and calponin (D~F) in red, F-actin in green with alexa(388)-rhodamine phalloidin. The micrographs (magnification, ×100) shown in this figure are representative of three independent experiments with similar results.

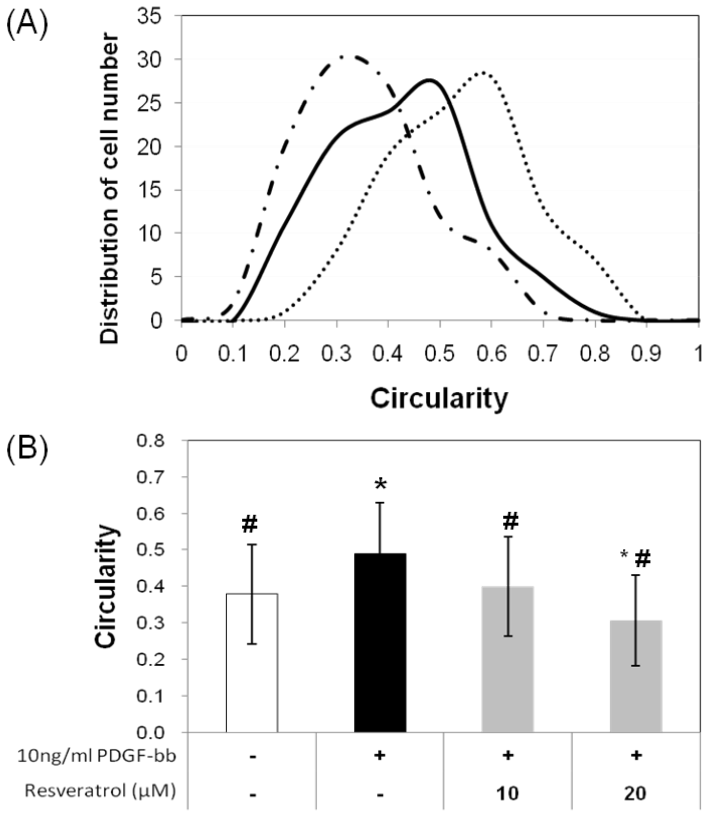

Figure 3-5. Morphology modulation of resveratrol on PDGF-bb stimulated RAOSMC. (A) The distribution of circularity ranged from 0 to 1, linear to circular, respectively. (— in serum free, —•— in 10 ng/ml PDGF-bb, and ••••• in 10 ng/ml PDGF-bb with 20 μM resveratrol) (B) The average circularity ± SD was obtained from 100 single cells per each type. * $P < 0.05$, compared with non-stimulation control; # $P < 0.05$ compared with 10 ng/ml PDGF-bb stimulated control.

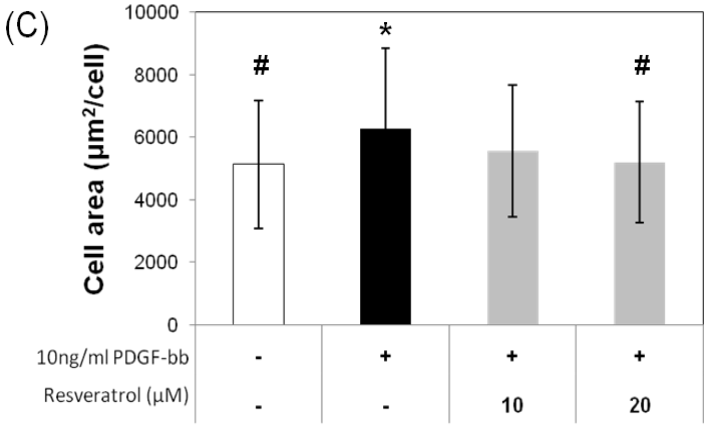

Figure 3-5. (continue) (C) The average area (μm^2/cells) ± SD was obtained from 100 single cells per each type. *P < 0.05, compared with non-stimulation control; # P < 0.05 compared with 10 ng/ml PDGF-bb stimulated control.

D. Inhibitory effect of resveratrol against PDGF-bb stimulated signal transduction pathways on RAOSMC

To define effect of resveratrol on signaling pathways involved in PDGF-bb stimulated dedifferentiation, serum starved cell were stimulated with 10 ng/ml PDGF-bb in the absence or presence of resveratrol for the indicated time. And then, we analyzed the activation of p42/44MAPK, p38MAPK, and Akt, a downstream effector of the PDGF-bb induced signaling by Western blotting.

Addition of 10 ng/ml PDGF-bb to serum-starved cells led to a complete PDGFR-β phosphorylation which peaked within 10 min and returned to baseline levels at 2~4 h and showed similar results at least three independent experiments (Fig. 3-6A). However, resveratrol inhibited PDGFR-β phosphorylation induced by PDGF-bb at only 10 min, while no inhibition of PDGFR-β phosphorylation was observed during incubation more than 30 min.

In a similar manner, PDGF-bb stimulated the phosphorylation of downstream effectors such as MEK1/2, p42/44MAPK (Fig. 3-6B), and p38 (Fig. 3-6C), whereas reveratol did not trigger the phosphorylation of MEK1/2, p42/44MAPK, and p38MAPK by PDGF-bb stimulation in time-dependent manner. However, as shown in Fig. 3-6D, Akt and mTOR phosphorylation upon PDGF stimulation elicited a strong and detectable signal for several hours, while resveratrol inhibited and induced only weakly the Akt phosphorylation and mTOR phosphorylation, downstream effector dependent on Akt.

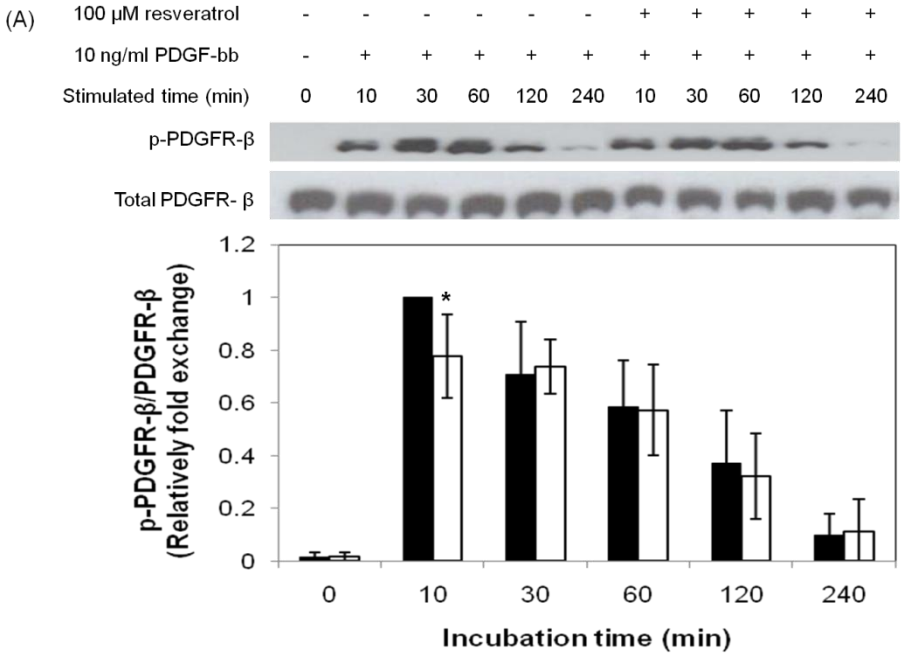

Figure 3-6. The effect of resveratrol on modulation of PDGF-bb stimulatory signal pathways in RAOSMC. RAOSMC starved serum were stimulated with 10 ng/ml PDGF-bb and 100 μM resveratrol for desired time (10 m, 30 m, 1 h, 2 h, and 4 h, respectively), lysed, and lysates were immunoblotted with antibodies. After densitometric quantification using imgaJ program, data were each expressed as the mean ± SD from three independent experiments. Black bar indicate expression by PDGF-bb stimulation. White bar indicate expression by PDGF-bb stimulation with EGCG. (A) The expression of phosphor PDGFR-β time dependent manner. The band intensity was normalized to PDGFR-β expression.

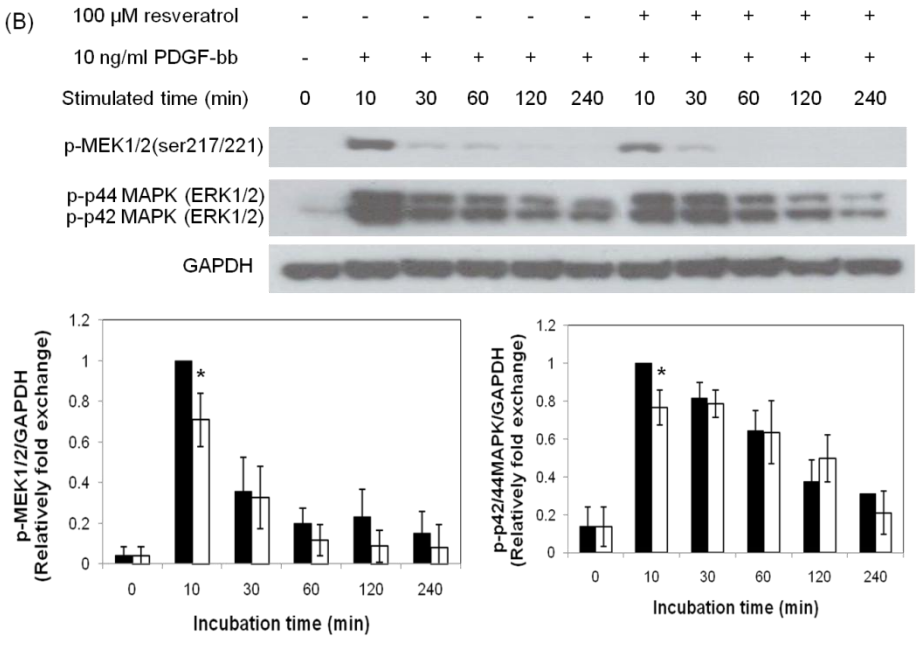

Figure 3-6. (continued) (B) The expression of phosphor MEK1/2 and phosphor p42/44MAPK on time dependent manner. The band intensity was normalized to GAPDH expression.

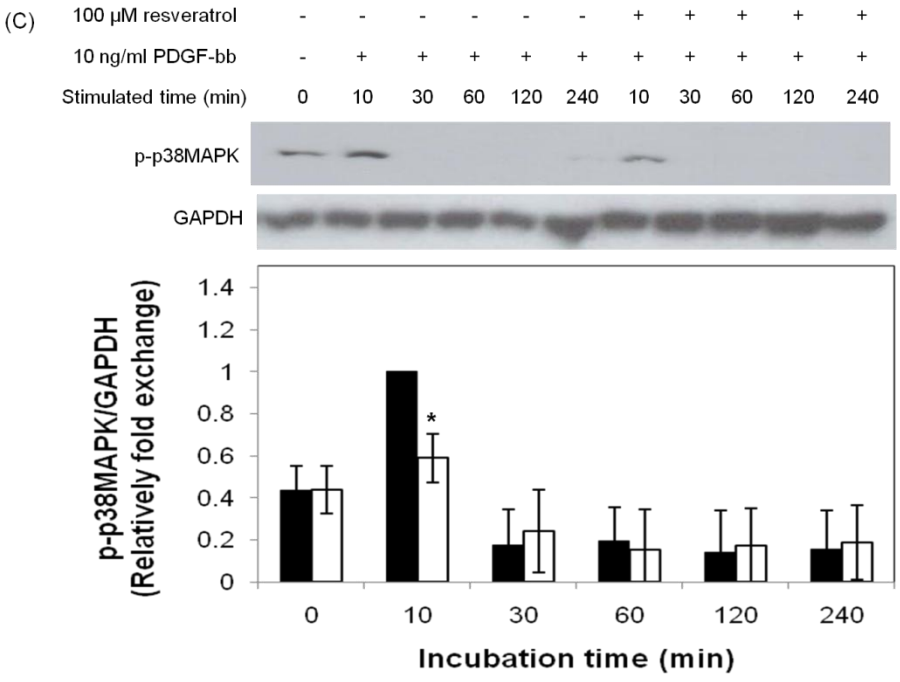

Figure 3-6. (continued) (C) The expression of phosphor p38 MAPK on time dependent manner. The band intensity was normalized to GAPDH expression.

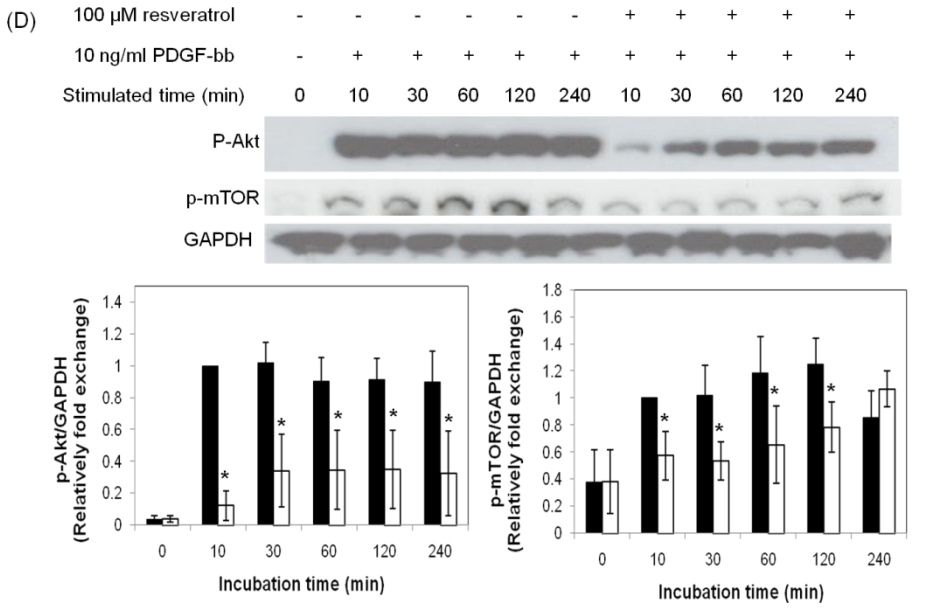

Figure 3-6 (continued) (D) The expression of phosphor Akt and phosphor mTOR on time-dependent manners. The band intensity was normalized to GAPDH expression.

4. Discussions

Alternations in the differentiated state of the VSMC play a critical role in the pathogenesis of major human diseases, as well as atherosclerosis, hypertension, asthma, and vascular aneurisms. Dedefferentiation of VSMC was based on morphological criteria, that terms “phenotypic modulation” or “phenotypic switching” in functional and structural properties. A phenotypic switch from a contractile to synthetic phenotype accompanies the proliferation and migration. PDGF-bb represses VSMC marker gene expression mainly through an extracellular signal-regulated kinase 1/2–mitogen activated protein kinase (ERK1/2-MAPK), p38 MAPK, and Akt pathway [16].

Polyphenols contribute to the vasoprotective, antiangiogenic, antiatherogenic, vasorelaxant and antihypertensive effects of acute or chronic administration of plant polyphenols found in patients[17]. Resveratrol, one of polyphenol compounds, blocks specifically PI3K/PDK1/Akt pathway, thereby inhibiting oxLDL induced SMC proliferation [13].

This study reported that the dedifferentiated VSMCs by PDGF-bb could undergo phenotypic changes by p42/44 MAPK, p38 MAPK, and Akt pathway trigger PDGFR-β on RAOSMC. In our experimental system, resveratrol inhibited proliferation of PDGF-bb stimulated RAOSMC. Also, contractile morphology, spindle phenotype, was preserved by resveratrol treatment in comparison with PDGF-bb stimulated RAOSMC. Therefore, differentiated VSMC marker such as αSMA and calponin was not inhibited. In other words,

resveratrol might prevent morphology change from contractile to synthetic phenotype.

VSMC in mature animal vessels exhibit a contractile phenotype (differentiated state), and express multiple contractile proteins, including αSMA, SM22α, SM-MHC, and so on [18]. Calponin and including αSMA is characterized in detail as an F-actin binding component of smooth muscle thin filaments and controlled actin-based cellular processes by regulating the stability of the actin cytoskeleton [6].

In investigation of signal transduction from PDGF-bb, resveratrol inhibited PDGFR-b, 42/44 MAPK, Akt and p38MAPK phosphorylation. Especially, Akt/mTOR phosphorylation was preferably inhibited in PDGF-bb induced cell stimulation by resveratrol. It is known that VSMC phenotype is determined by changes in the balance between the Akt pathway and the ERK and p38MAPK pathways. PDGF-bb triggers the dual signaling pathways, PI3-K/PKB (Akt) and two MAPKs. Therefore, the phosphoinositol-Akt-mammalian target of rapamycin-p70S6 kinase (PI3K/Akt/mTOR/p70S6K) pathway regulates cell growth and cell differentiation in response to nutrients, growth factors, and cytokines [19]. Pharmacological rapamycin induces contractile morphology and SM2-MHC and calponin, and reduced protein and collagen synthesis in cultures of synthetic phenotype VSMCs by regulation of mTOR/p70 S6K1 pathway [20]. The previous data show that mTOR activation induced SMC proliferation and requires the activation of the signaling cascade PI3K/PDK1/Akt, as assessed by

the effect of the PI3K inhibitors wortmannin and Ly294002 that block PDK1 [9,10,21].

In this study, we have focused effect of resveratrol on phenotypic modulation following stimulation by PDGF-bb on RAOSMC. From a general point of view, resveratrol exhibits various potentially inhibitory properties of dedifferentiation, including anti-proliferation effect and an ability to modulate major signaling pathways.

5. Conclusion

In this study we investigated the effect of resveratrol on didiferentiation of RAOSMC induced by PDGF-bb. Resveratrol inhibited the PDGF-bb stimulated proliferation, MMP secretion and phenotype change from contractile morphology to synthetic morphology on RAOSMC. This result was explained expression of contractile phenotype related protein and Akt/mTOR signal pathway. In conclusion, our results indicate that RAOSMC dedifferentiation, phenotype and proliferation rate were inhibited by resveratrol by interrupting the balance of the Akt and 42/44MAPK and p38MAPK pathway activation stimulated by PDGF-bb. This result can suggest that resveratrol may be inhibitor of phenotype modulation occurring in arterial stenosis and in postangioplasty restenosis on vascular injury.

6. Reference

1. Davies MG, Hagen PO. Pathobiology of intimal hyperplasia. Br J Surg 1994; 81:1254-69.
2. Coats WD, Faxon DP. The role of the extracellular matrix in arterial remodelling. Semin Intervent Cardiol 1997; 2:167-76.
3. Schwartz SM. Smooth muscle migration in atherosclerosis and restenosis. J Clin Invest 1997; 99:2814-7.
4. Kenji S, Ken'ichiro H, Wataru N. Molecular Mechanism of Phenotypic Modulation of Smooth Muscle Cells. Horm Res 1998;50(suppl 2):15–24.
5. Rzucidlo EM, Martin KA, Powell RJ, Lebanon NH. Regulation of vascular smooth muscle cell differentiation. J Vasc Surg 2007;45:25A-32A.
6. Rozenblum GT, Gimona M. Calponins: Adaptable modular regulators of the actin cytoskeleton The International Journal of Biochemistry & Cell Biology 2008;40:1990–5.
7. Heldin CH, Westermark B. Mechanism of action and in vivo role of platelet-derived growth factor. Physiol Rev 1999;79:1283–16.
8. Zhan Y, Kim S, Izumi Y, Izumiya Y, Nakao T, Miyazaki H, et al. Role of JNK, p38, and ERK in Platelet-Derived Growth Factor–Induced Vascular Proliferation, Migration, and Gene Expression. Arterioscler Thromb Vasc Biol 2003;23;795-801.
9. Sekulic A, Hudson CC, Homme JL, Yin P, Otterness DM, Karnitz LM, et al. A direct linkage between the phosphoinositide 3-kinase-AKT signaling

pathway and the mammalian target of rapamycin in mitogen-stimulated and transformed cells. Cancer Res 2000;60:3504–13.

10. Wullschleger S, Loewith R, Hall MN. TOR signaling in growth and metabolism. Cell 2006;124:471–84.
11. Sadruddin S, Arora R. Resveratrol: biologic and therapeutic implications. J Cardiometab Syndr 2009;4(2):102-6.
12. Wang XB, Huang J, Zou JG, Su EB, Shan QJ, Yang ZJ, et al. Effects of resveratrol on number and activity of endothelial progenitor cells from human peripheral blood. Clin Exp Pharmacol Physiol 2007;34(11):1109-15.
13. Brito PM, Devillard R, Nègre-Salvayre A, Almeida LM, Dinis TC, Salvayre R, et al. Resveratrol inhibits the mTOR mitogenic signaling evoked by oxidized LDL in smooth muscle cells. Atherosclerosis. 2009;205(1):126-34.
14. Sung HJ, Eskin SG, Sakurai Y, Yee A, Kataoka N, McIntire LV. Oxidative stress produced with cell migration increases synthetic phenotype of vascular smooth muscle cells. Ann Biomed Eng 2005;33(11):1546-54.
15. Li S, Sims S, Jiao Y, Chow LH, and Pickering JG. Evidence from a novel human cell clone that adult vascular smooth muscle cells can convert reversibly between noncontractile and contractile phenotypes. Circ Res 1999;85:338–48.
16. Kawai-Kowase K, Owens GK. Multiple repressor pathways contribute to phenotypic switching of vascular smooth muscle cells. Am J Physiol Cell

Physiol 2007;292(1):C59-69.

17. Stoclet JC, Chataigneau T, Ndiaye M, Oak MH, El Bedoui J, Chataigneau M, et al. Vascular protection by dietary polyphenols. Eur J Pharmacol 2004;500:299–313.
18. Owens GK, Wise G. Regulation of differentiation/ maturation in vascular smooth muscle cells by hormones and growth factors. Agents Actions Suppl 1997;48:3–24.
19. Corradetti MN, Guan KL. Upstream of the mammalian target of rapamycin: do all roads pass through mTOR? Oncogene 2006;25: 6347–60.
20. Martin KA, Rzucidlo EM, Merenick BL, Fingar DC, Brown DJ, Wagner RJ, et al. The mTOR/p70 S6K1 pathway regulates vascular smooth muscle cell differentiation. Am J Physiol Cell Physiol 2004;286: C507-17.
21. Auge N, Garcia V, Maupas-Schwalm F, Levade T, Salvayre R, Negre-Salvayre A. Oxidized LDL-induced smooth muscle cell proliferation involves the EGF receptor/PI-3 kinase/Akt and the sphingolipid signaling pathways. Arterioscler Thromb Vasc Biol 2002;22:1990–5.

IV. PERIADVENTITIAL APPLICATOON FOR DELIVERY OF EPIGALLOCATECHIN-3-O-GALLATE AND RESVERATROL BY ELECTROSPUN POLY(L-LACTIDE GLYCOLIC ACID) FIBER SHEETS TO REDUCE INTIMAL HYPERPLASIA AFTER ABDOMINAL AORTA BALLOON INJURY IN RABBIT

1. Introduction

Intimal hyperplasia (IH) is the major cause of failure in invasive treatments for vascular diseases, arterial catheter based and endovascular surgical intervention. It occurs in response to endothelium injury of intimal layer, including balloon angioplasty, stent placement, or graft implantation. After all, vascular damage leads vascular thickness and narrowing by inducing the migration and proliferation of phenotype modulated VSMC, and vascular remodeling. Over the years a number of treatment strategies have evolved to prevent or inhibit intimal hyperplasia. Alternative treatments have evolved to inhibit of IH that would lead to better efficacy. These include locally pharmacological therapy such as drug eluting balloon catheter and drug delivery stents.

Polymeric local drug delivery systems have been studied for cancer chemotherapy and cardiovascular therapy such as in stents, catheters for preventing of restenosis. A controlled and site-specific drug therapy is able to improve therapeutic efficacy, reduce side toxicity and can be designed to control and prolong drug release by adjusting the degradation rate of the polymer [1,2].

Furthermore, novel formulations using degradable polymer were developed

such as nanoparticles, microemulsions, matrix systems, solid dispersions, liposomes, solid lipid nanoparticles and so on, for delivery of the components in a sustained manner to increase patient compliance and avoid repeated administration [3].

Electrospinning is a technique to produce continuous polymeric fibers with porosity from a variety of polymers and composite materials that utilizes high voltage source. As a potential drug delivery carrier, electrospun fibers have exhibited many advantages. Electrospun fiber is very easy to load soluble and insoluble drugs for enhancing their dissolution according to solvent change, and the high applied voltage had little influence on the drug activity. Therefore, it allows better control of release than bulk materials by modulation of fiber morphology, porosity and composition [4]. In particular, poly(lactic-co-glycolic acid) (PLGA) has been extensively used for a controlled drug delivery system because its polymer chains are cleaved by hydrolysis into natural metabolites (lactic and glycolic acids) and it offers a wide range of degradation rates, from months to years, depending on its composition and molecular weight [5,6].

Our previous study was investigated that epigallocatechin-3-gallate (EGCG), major component of green tea polyphenol, is a very potent anti-proliferative molecule that inhibits mitogenesis by downregulation of MPAK. Local delivery of green tea catechin following endothelial denudation prevented neointimal formation in balloon injured rat carotid model [7]. Resveratrol, a polyphenol present in wine and in various foods, inhibit phenotype modulation by the

dedifferentiation of VSMC. Therefore, resveratrol administration inhibited intimal hyperplasia after endothelial denudation in an experimental [8].

In the present study, we were to develop a polymeric local drug delivery device by electrospun methods for delivery of EGCG and resveratrol with PLGA polymer. Therefore, we investigated whether perivascularly local delivery device contained EGCG and resveratrol that wrapped around the sites of vascular damage inhibited intimla hyperplasia and prevented luminal narrowing in endothelium denuding rabbit model by balloon injury.

2. Materials and Methods

A. Fabrication of polyphenol release PLGA sheet and physicochemical characterization

(A) Fabrication of polyphenol eluting PLGA sheet

PLGA(75:25(mol/mol), 113000 molecular weight (MW))was purchased from Lakeshore Biomaterials (Birmingham, AL, USA). PLGA was prepared by dissolving in tetrahydrofuran (THF, Sigma)/ Dimethyl formamide (DMF, Sigma) (4:1) to obtain 20% w/w solution, EGCG (Teavigo™, DSM Nutritional Products Ltd., Basel, Switzerland) and resveratrol (Terraternal, Santa Clara, CA, USA) was added to the solution to 40% and 50% volume of PLGA, respectively. PLGA sheets were fabricated at 9.5 kV using a high voltage DC supply at 25℃, 35% humidity. The ground collection plate was located at a fixed distance of 10 cm the needle tip and the flow rate was controlled in 1 ml/h. The polyphenol eluting PLGA sheet was all dried for 24 h at room temperature. Upon completion of the spinning process, the nonwoven electrostatically spun fabric was removed from the collector

(B) Field Emission Scanning Electron Microscopy (FE-SEM)

The surface topography of the electrospun PLGA fibers was assessed under a field emission scanning electron microscope (Hitachi S-800, Tokyo, Japan).

EGCG and resveratrol eluting electrospun fiber sheets were mounted and sputter coated with platinum using an ion coater. Coated fibers were placed in the microscope chamber to which a high vacuum was applied. Histograms of fiber diameter were generated by the measurement in 4000 x.

(C) Attenuated total reflectance/Fourier transform-infrared (ATR/FT-IR) spectroscopy

The infrared spectra of polyphenol eluting PLGA sheets were performed using an ATR/FT-IR spectrophotometer (Spectrum 100, Perkin elmer, Shelton, CT, USA) and obtained between 5000 and 600 cm^{-1} at room temperature. Samples, PLGA sheet, polyphenol eluting PLGA sheets, EGCG powder, and resveratrol powder, were placed on holder and mounted in the enclosed sample chamber, away from moisture to get their spectra, respectively.

(D) In vitro release profile of EGCG and resveratrol from polyphenol eluting PLGA sheet

Polyphenol eluting PLGA sheet was prepared in 1cm X 1cm and then incubated in 5ml phosphate-buffered saline (PBS, pH7.4) at 37℃ with shaking at 224 rpm for up to 40 days. At the end of each predetermined incubation period, solution absorbance of EGCG and resveratrol from released buffer were determined by a UV-Vis spectrophotometer (Shimadzu UV-1800, Shimadzu Corporation, Tokyo, Japan) and calculated from the standard calibration curve of EGCG and

resveratrol solution in PBS. Each measurement was performed in triplicate (n=3) and the values averaged. To determine the actual amount of EGCG and resveratrol eluting PLGA sheets, 1cm x 1cm sheet were weighed and dissolved in DMSO, then the solution was diluted and performed by a UV-Vis spectrophotometer (Shimadzu UV-1800), and calculated from the standard calibration curve of EGCG and resveratrol solution in DMSO, respectively.

B. External application of polyphenol eluting PLGA sheet on aorta

(A) Animal model

All animal experiments were performed with the "Guide for the Care and Use of Laboratory Animals" and a protocol approved by the Animal Care and Use Committee of Yonsei University College of Medicine.

Male New Zealand White rabbits, weighing 3 to 3.5 kg, were anesthetized with intramuscular and intravenous injections of Zoletile (15 mg/kg, Boehringer Ingelheim Agrovet, Hellerup, Denmark) and Rompun (5 mg/kg, Bayer, Toronto, Canada).

After intravenous administration of heparin 1000 U/kg, the abdominal aorta was exposed and the distal femoral arteries were exposed and ligated. A 3F Fogarty embolectomy catheter (Edwards lifescience, Irvine, CA, USA) was inserted via a left femoral arteriotomy and passed 20 cm into the abdominal aorta. The catheter was inflated and drawn back to the iliac bifurcation. Catheter insertion

and inflation were repeated for three passes, after which the catheter was removed, the femoral artery was tied, and the incision was closed (Fig. 4-1).

Polyphenol eluting PLGA sheet was prepared to 1cm x 3cm and sterilized 1 kG / hr for 25 h by γ- irradiation. Polyphenol eluting PLGA sheet was wrapped to twister direction at balloon injury sites on abdominal aorta. Experimental groups were divided into the PLGA sheet group (n=5), EGCG eluting PLGA sheet group (n=5), and resveratrol eluting PLGA sheet group (n=3). All animals were allowed to recover and returned to routine care. Animals were maintained on a normal laboratory diet and were euthanized 4 weeks after operation.

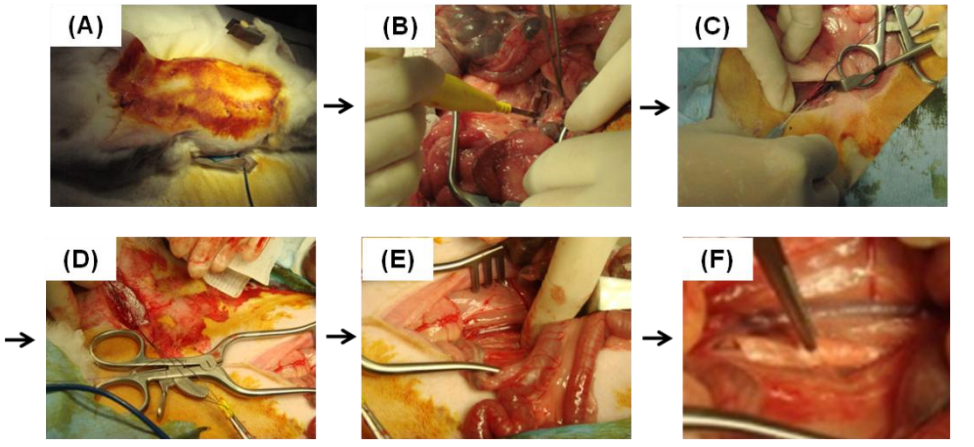

Figure 4-1. Surgical procedure of ballon injured model in rabbit abdominal aorta. New Zealand white rabbit was anesthetized (A), expose of abdominal aorta (B), inserted of balloon catheter through femoral artery (C,D), injured of abdominal aorta (E), and wrapped of electrospun PLGA fiber sheet (F).

(B) Histology analysis

In order to quantify neointimal hyperplasia, rabbits were sacrificed at 4 weeks after the balloon injury. The rabbit were administrated in intravenous of heparin 1000 U/kg and isolated. The aorta was harvested and removed of wrapped sheet, and fixed in 10% neutral buffered formalin for 1 d. Vessels were processed and embedded in paraffin block. Sections 5–6 μm thick were cut on a rotary microtome and collected on glass slides. Adjacent sections were stained with hematoxylin and eosin (H&E), and measured of intimal and medial area using imageJ software (National Institutes of Health, Bethesda, Maryland, USA).

3. Results

A. Fiber morphology of polyphenol eluting PLGA sheet

To determine the morphology of the spun fibers, an analysis of FE-SEM images was performed. The entire appearances of the EGCG and resveratrol eluting PLGA fiber sheet were observed red and yellow color, EGCG and resveratrol, respectively (Fig. 4-2A~C). The electrospun PLGA fibers had typical fiber mat and a bead-free fibrous structure whether in the presence or absence of EGCG or resveratrol. As illustrated in Fig. 4-3, PLGA fiber were generated with a diameter of 1.2 μm to 2.8 μm, 1.7 μm to 2.9 μm for the 40% EGCG eluting fibers, and 1.5 μm to 2.6 μm for the 50% resveratrol eluting fibers. After 30 d under physiological conditions at 37 ℃, electrospun PLGA fiber sheet had decreased in size by 50 % of original area (Fig. 4-2A, D). Therefore, immediately after electrospinnig, the fibers looked fairly straight with ample space in between individual fibers. After incubation in PBS at 37 ℃, the fibers were revealed appearance to considerable shrinkage. Therefore, fibers appeared bulkier and considerably closer together with the elimination of space between the fibers (Fig. 4-3A, D).

As shown Figure 4-2E, EGCG eluting electrospun PLGA fiber sheet after incubation in PBS at 37 ℃ for 30 d, sheet size decreased to 50 % of original area. However, fiber appearance was not changed and observed pores and damage in fiber, which by EGCG release (Fig. 4-3K). While the size change of

resveratol eluting electrospun PLGA fiber was not observed, the edge of sheet was round form (Fig. 4-2F). As illustration in Fig. 4-3L, sheet was observed the damage and pores of fibers by polymer degradation and resveratrol release.

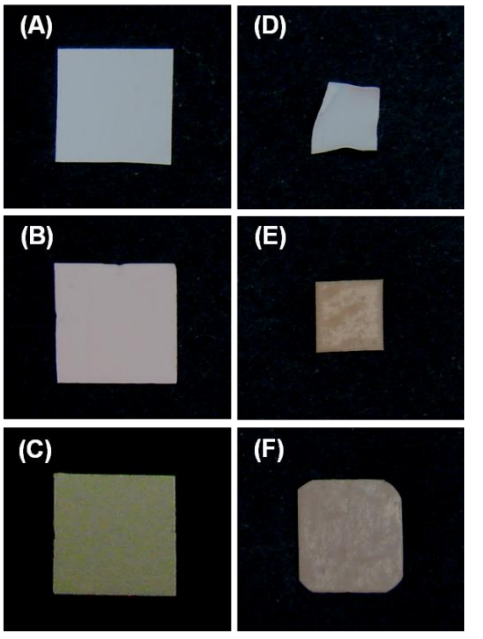

Figure 4-2. The entire appearance of electropun PLGA fiber sheet (A,D), EGCG eluting PLGA sheet (B, E), and resveratrol eluting PLGA sheet. (A~C) immediately photography after electrospining, (D~F) photography of sheet after incubation in PBS at 30 ℃ for 30 d.

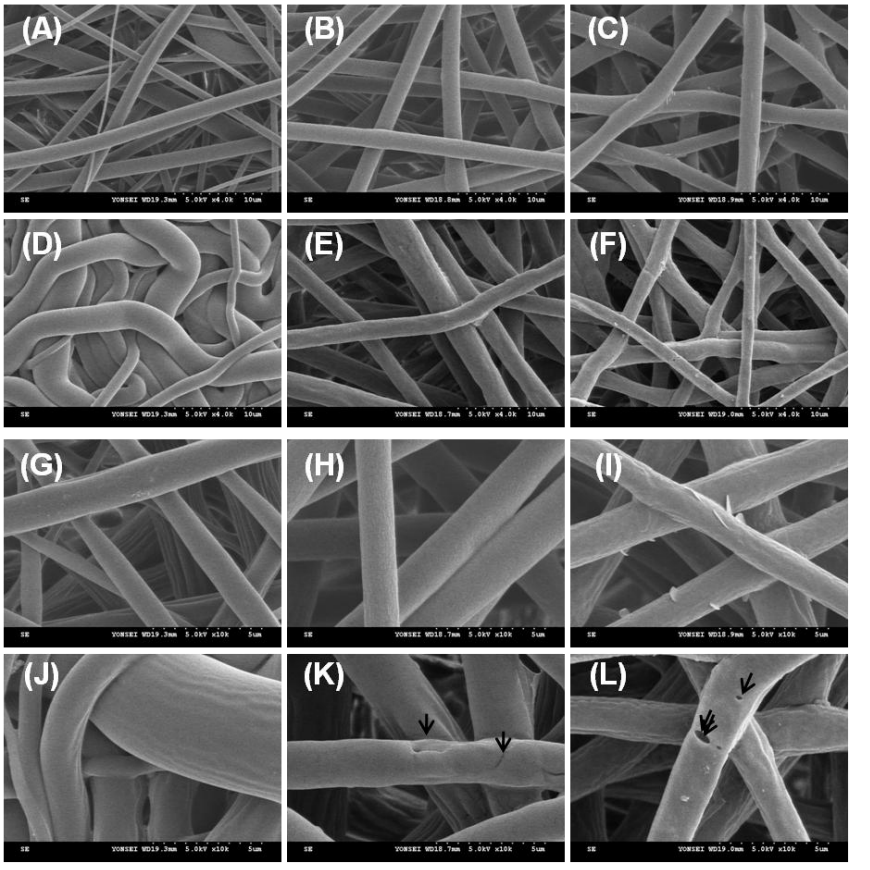

Figure 4-3. SEM micrographs on electrospun PLGA fibers (A,G) at 0 days, and (D,J) after incubation in PBS at 30 ℃ for 30 days EGCG eluting PLGA fibers (B,H), at 0 day, and (E,K) after incubation in PBS at 30 ℃ for 30 days. Resveratrol eluting PLGA fibers (C,I) at 0 day, and (F,L) after incubation in PBS at 30 ℃ for 30 days.

B. FTIR spectra of polyphenol eluting PLGA sheet

From the FTIR spectra, distinctive peaks of EGCG and resveratrol were observed from spectra of their respective EGCG or resveratrol eluting PLGA sheet. The FTIR spectra of EGCG eluting electroepun PLGA fiber are shown in Figure 4-4. Distinctive peaks at 3600–3150 cm^{-1} (phenyl-OH) were observed from EGCG eluting sheet. Additionally, the characteristic bands of EGCG were found at 1610 $cm^{-1}$for C=C alkenes and at 823 cm^{-1} for C–H alkenes.

Resveratrol eluting electrospun PLGA fiber sheet was also dominated by a broad notable band at 3600–3150 cm^{-1} (phenyl-OH), which is the characteristic peak of phenyl-OH groups abundant in resveratrol. Therefore, peak at 1770 cm^{-1} (C=O) and1660 cm^{-1}(C=C) were observed from sheet (Fig. 4-5).

This indicated that EGCG or resveratrol were successfully loaded and dispersed into PLGA sheets.

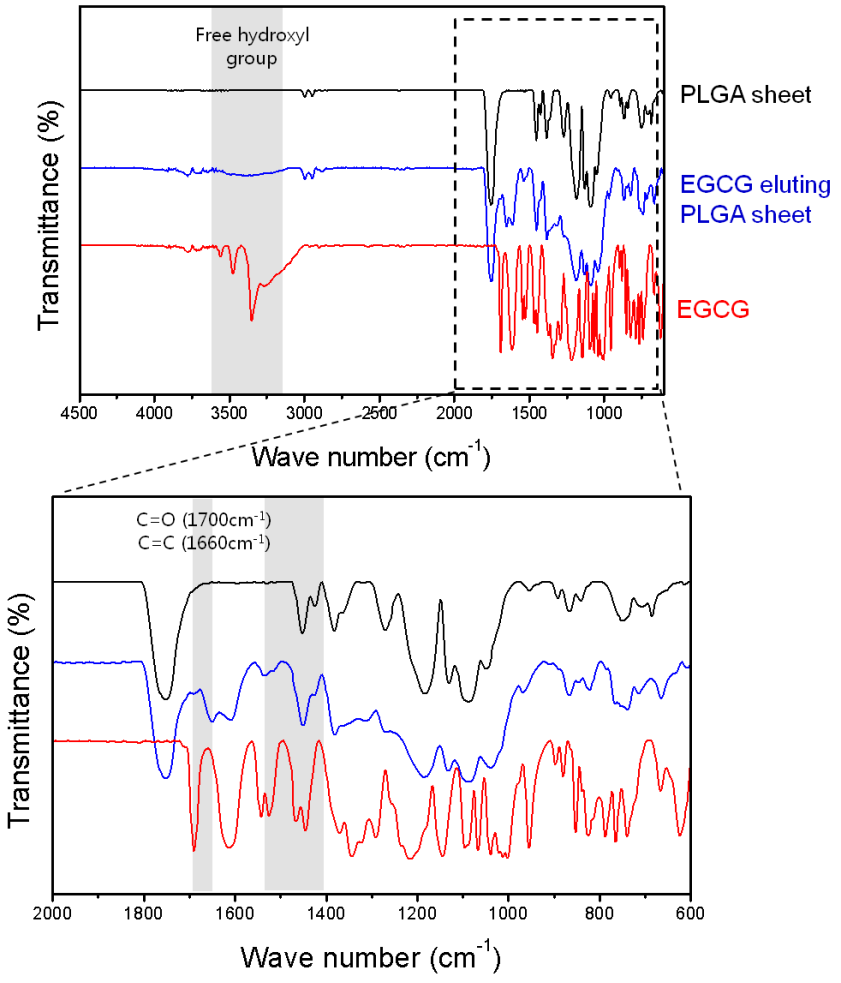

Figure 4-4. FT-IR spectra of PLGA sheet (upper line), EGCG eluting PLGA fiber (middle line), and only EGCG (bottom line). Upper spectra revealed between 5000 and 600 cm^{-1}, and bottom spectra obtained between 2000 and 600 cm^{-1}.

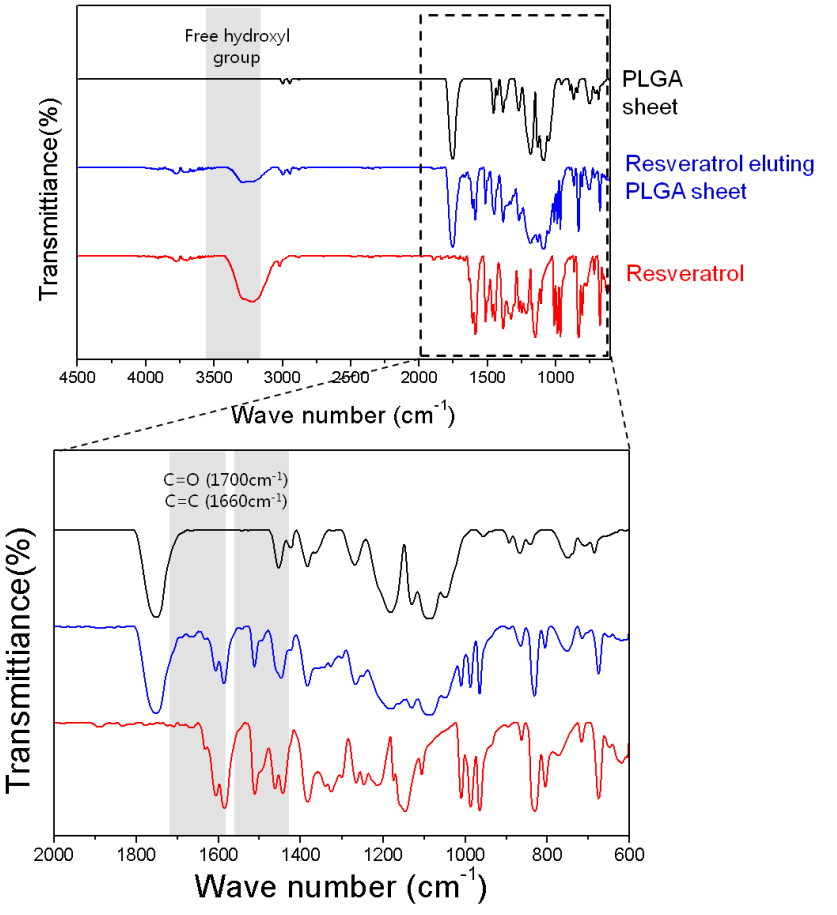

Figure 4-5. FT-IR spectra of PLGA sheet (upper line), resveratrol eluting PLGA fiber (middle line), and only resveratrol (bottom line). Upper spectra revealed between 5000 and 600 cm^{-1}, and bottom spectra obtained between 2000 and 600 cm^{-1}.

C. EGCG Release from EGCG eluting electrospun PLGA sheet

To study the release of the incorporated EGCG from electrospun PLGA sheet, EGCG amount was determined by UV/VIS spectrophotometer. The wavelength of maximal absorbance of EGCG in PBS solution was detected 275nm (Fig. 4-6 A). Dissolution of EGCG in PBS was a linear increase in the absorbance of EGCG solutions, more than 200 μg/ml, after which the absorbance remained constant, this concentration corresponds to the limit of solubility of EGCG UV/VIS spectra (Fig. 4-6B). The EGCG on EGCG eluting PLGA sheet were contained 1641.2 ± 377.4 μg per 1 x 1cm sheet and found to be 80~90 % of input amount for sheet fabrication. The release characteristics were carried out in phosphate buffer saline at 37 ℃. The cumulative amount of the drug released from the drug-loaded fibers is illustrated in Fig. 4-6C. Total EGCG amount was determined prior to the release studies to calculate the release percentage of the actual EGCG amount of sheet. EGCG eluting electrospun PLGA fiber sheet showed an initial burst release of about 80% within a 1 day upon contact with PBS solution, then, followed by sustained release up to 40 days from EGCG eluting PLGA sheets.

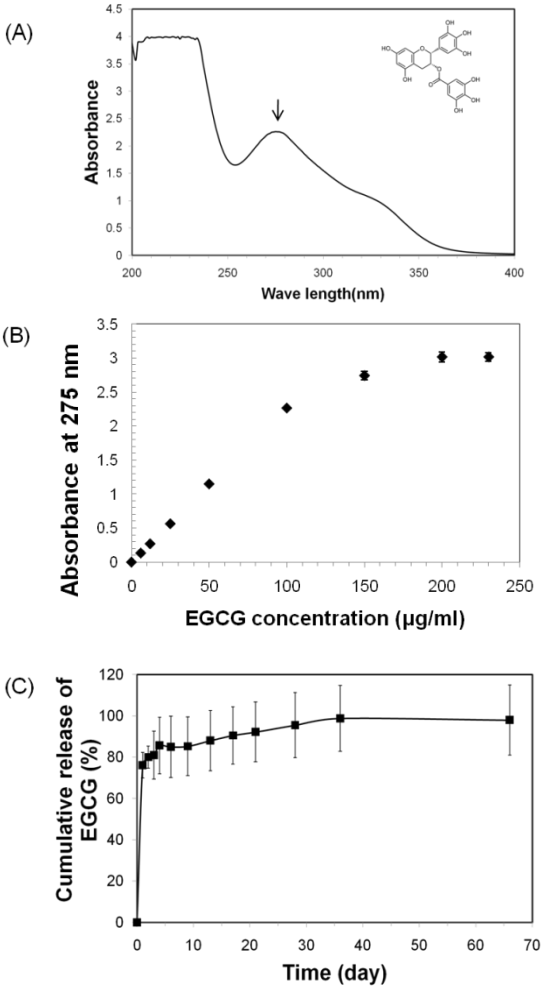

Figure 4-6. *In vitro* EGCG release of EGCG eluting electrospun PLGA fiber sheet. (A) Absorbance spectrum of a 100 μg/ml EGCG in PBS solution by UV/VIS spectrophotometer. (B) Absorbance at 275 nm as a function of the concentration of EGCG solution in PBS. Results are expressed as mean ± SD deviation of three experiments. (C) Accumulative release profile of EGCG up to 70 days

D. Resveratrol release from resveratrol eluting electrospun PLGA sheet

To study the release of the incorporated resveratrol from electrospun PLGA sheet, resveratrol amount was determined by UV/VIS spectrophotometer. The wavelength of maximal absorbance of rsveratrol in PBS solution was detected 311nm (Fig. 4-7A). Dissolution of resveratrol in PBS was a linear increase in the absorbance of resveratrol solutions, up to 30 μg/ml (Fig. 4-6B). The resveratrol on resveratrol eluting PLGA sheet were contained 1767.1 ± 109.6 μg per 1x1cm sheet and found to be 90 % of input amount for sheet fabrication. The release characteristics were carried out in phosphate buffer saline at 37 ℃. As shown in Figure 4-7C, resveratrol was released in a logarithmic manner up to 20 days after which the release rate decreased with time.

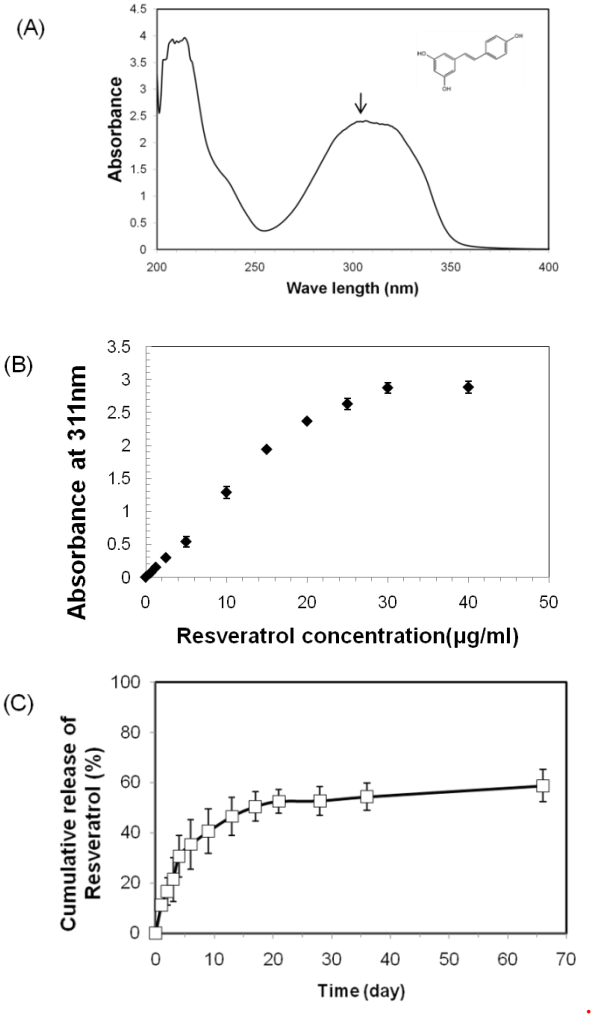

Figure 4-7. *In vitro* release profile of resveratrol from resveratrol eluting electrospun PLGA fiber sheet. (A) Absorbance spectrum of a 20 μg/ml resveratrol in PBS solution by UV/VIS spectrophotometer. (B) Absorbance at 311 nm as a function of the concentration of resveratrol solution in PBS. Results are expressed as mean ± SD deviation of three experiments. (C) Accumulative release of resveratrol up to 70 days.

E. Effect of intimal formation by externally application of polyphenol eluting PLGA sheet at balloon injured abdominal aorta on rabbit

We investigated the effect of locally administered EGCG and resveratrol on neointima formation at day 28 post injury, respectively. Representative photomicrographs of hematoxylin–eosin stained sections of treated and control arteries are shown in Fig. 4-8. After balloon injury, lumen was expanded and internal elastic lamina (IEL) was injured (Fig. 4-8 A,B). Balloon injury of the aorta decreased in luminal area and exhibited intimal hyperplasia at 28 days after injury (Fig. 4-8C). Morphometric analysis revealed significantly decreased intima/media (I/M) ratio in EGCG eluting electrospun PLGA fiber sheet (Fig. 4-9). We found a significantly ($p<0.05$) 30% and 50% reduction of intimal area in wrapped aorta with EGCG and resveratrol, respectively (Fig. 4-9A). The medial area was not significantly by EGCG and resveratrol treatment in comparison with vehicle PLGA control. Compared to vehicle controls, we found significant inhibition of 32% (EGCG) and 46% (resveratrol) of intimal/medial ration, respectively (Fig. 4-9B).

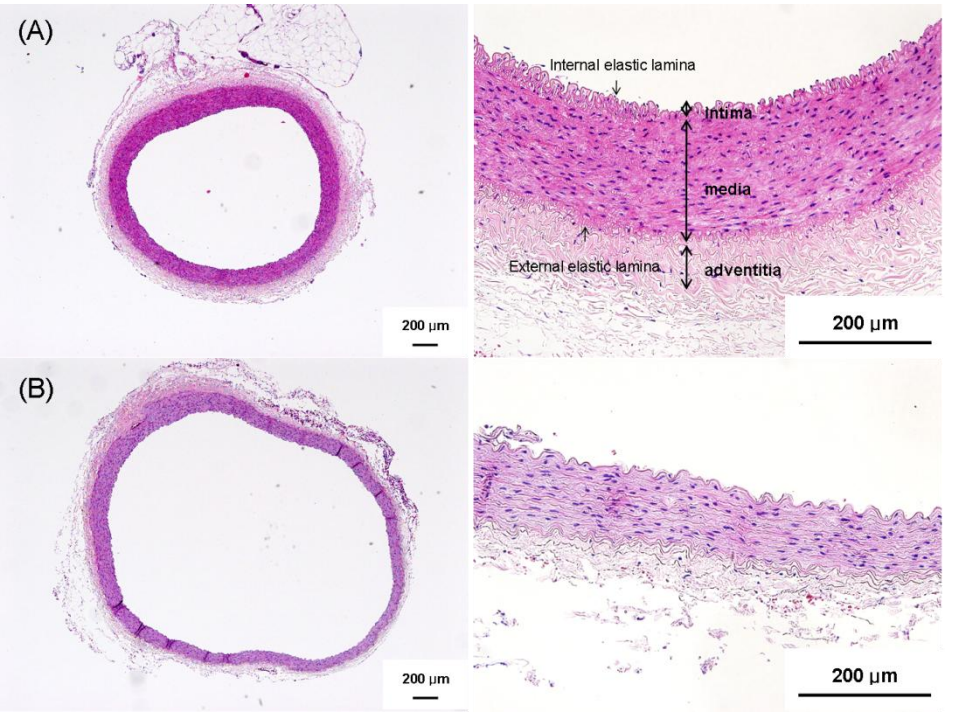

Figure 4-8. Representative photomicrographs of H&E stain on rabbit aorta cross-sections. Bar represent 200 μm. Right panels were observed at 20x magnifications, and left panels were observed at 200x magnifications. (A) Normal aorta (B) Aorta after balloon injury

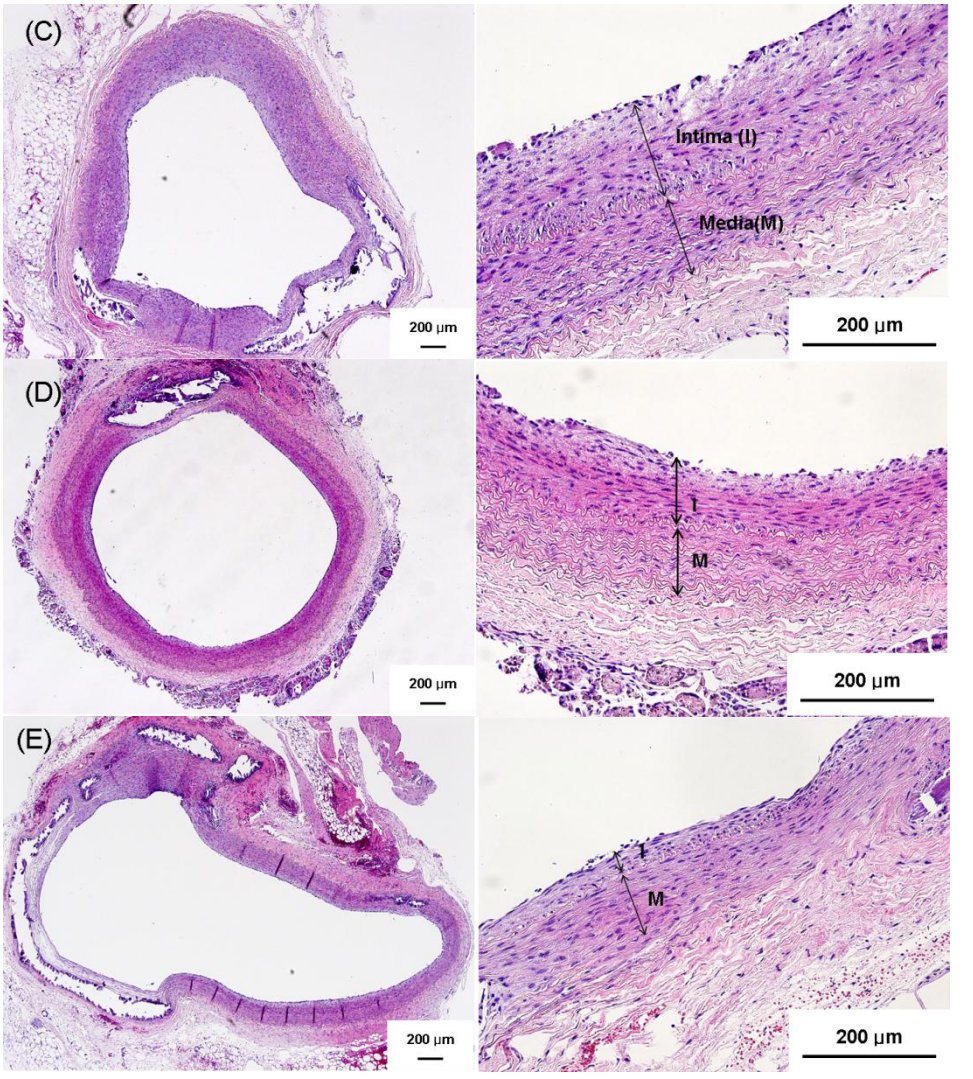

Figure 4-8. (continued) (C) Wrapped aorta with electrospun PLGA fiber sheet for 4 weeks after balloon injury (D) Wrapped aorta with EGCG eluting electrospun PLGA fiber sheet for 4 weeks after balloon injury (E) Wrapped aorta with resveratrol eluting electrospun PLGA fiber sheet for 4 weeks after balloon injury

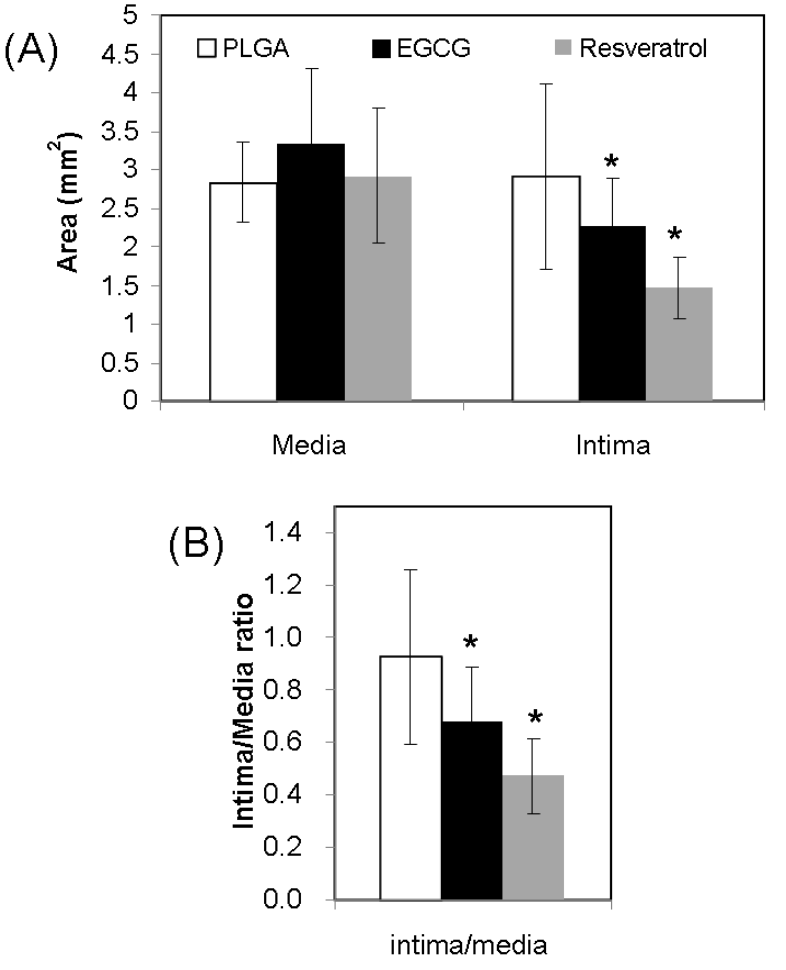

Figure 4-9. Morphometric analysis of intimal thickening in rabbit aorta 4 weeks after balloon injury. Intimal thickening is characterized by measuring the intimal area and the medial area to determine the intima/media ratio. The white bar represents electrospun PLGA fiber sheet. The black bar represents EGCG eluting sheet. The gray bar represents resveratrol eluting sheet. Results are expressed mean ± SD. (A) Area of intima and media (B) Intima/Media ratio *$P < 0.05$, compared with PLGA sheet.

4. Discussions

Effective treatment and control of vascular disease can be achieved by a regulation of abnormal VSMCs growth, and VSMC dedifferention. In this study, we implemented externally application of EGCG and resveratrol using electrospun biodegradable PLGA fiber sheet as delivery system for preventing effect of intimal hyperplasia. It has been reported in the literature that interactions between polymer and drug are known to govern the pattern of drug release from electrospun scaffolds.

In the present study, EGCG and PLGA eluting PLGA fiber sheet were prepared with uniformly dispersed EGCG as shown in picture and FT-IR spectrum (Fig. 1, 4-4, and 4-5). EGCG was released with a fast initial burst phase from EGCG eluting elctrospun PLGA fiber sheet (Fig. 4-6C), while resveratrol was released by sustained release phase (Fig. 4-7C). These may be different of water solubility between EGCG and resveratrol. As shown figure 4-6C, solubility of resveratrol was lower 7 times than EGCG, which EGCG was solved about 200 μg in 1ml PBS, but resveratrol was solved 30 μg. In case of hydrophilic drug and hydrophilic polymer an immediate and burst release is observed in comparison with hydrophobic drug and hydrophobic polymers with slowly release [9].

Prepared delivery system was application in adventitial surface in order to wrap the endothelium injured vessel. From the many studies conducted, it has been developed that the externally application sheath for perivasular delivery of

drugs using synthetic materials, remarkably decrease intimal hyperplasia and media thickening [10,11]. Previous study has shown that perivascular slow delivery of paclitaxel prevents luminal narrowing and inhibits intimal hyperplasia in balloon-injured rat carotid arteries [12]. Adventitial delivery of PD98059, inhibitor of mitogen-activated ERK kinase, from pluronic gel implanted adjacent to the injured artery in a rat model has demonstrated a reduction in neointimal formation [13]. Therefore, these result revealed inhibition effect of intima hyperplasia by adventitial delivery of heparin from a polymeric matrix in artery injured rat model [14,15].

In this study, we observed that externally wrap of EGCG and resveratrol eluting PLGA sheet inhibited thickness of intimal layer in balloon injury aorta of rabbit. However, inhibitory effect was grater in resveratrol system than EGCG. Although inhibitory mechanism is different between polyphenols, these may be related to release pattern. Therefore, it is harder to show what has better therapy effect in experimental study. An advantage of perivascular delivery is that the formulation is not in direct contact with blood, thus reducing the risk of thrombosis. However, efficacy of a drug applied to the outer surface of a blood vessel on a process taking place in the lumen remains to be demonstrated [16].

Recent studies have also implicated adventitia in the intimal hyperplastic response. The adventitia plays a role in the maintenance of the integrity of the inner layers of the arterial wall. Injury to the adventitia, and more particularly to the vasa vasorum, can induce intimal lesion formation despite an intact

endothelium in femoral arteries of pigs and rabbit[17,18]. Other animal models have shown that adventitial fibroblasts may migrate and proliferate in the intima within the first few days after arterial injury. These cells then undergo differentiation into myofibroblasts that express smooth muscle a-actin and synthesize extracellular matrix [19,20]. In addition, cell proliferation has been detected in the adventitia at an early stage after experimental angioplasty. These proliferating adventitial cells have been identified as myofibroblasts. They can migrate into the neointima and synthesize several components of the extracellular matrix [19,21-23]. These studies underscore the importance of adventitia in changes of the intima and the importance of vasa vasorum for vessel integrity and preserving lumen. Hence, the adventitia could be an important target site of local drug delivery that could prove instrumental in inhibiting IH.

This study was an initial experiment to access the feasibility and histopathologic effects of EGCG or resveratrol contained PLGA delivery system by periadventitia wrapping in balloon injured rabbit model. To evaluate the efficacy of this method need further studies, that determination of significant amount of polyphenol released from the polymers for reach the inner layers of the treated arteries and observation of EGCG and resveratrol concentration released from devices in treated vessel and blood, and inhibition study of intimal hyperplasia by long term implantation.

5. Conclusion

The purpose of this work was to demonstrate the feasibility of local application for sustained release of polyphenol eluting PLGA sheet prepared by electrospinning as an adventitial wrap for inhitition of intimal hyperplasia

In conclusion, EGCG and resveratrol released from sheets can suppress neointima formation through adventitial administration in injured arteries. From the therapeutic point of view, these results suggest that EGCG and resveratrol can be a potential agent for the prevention of VSMC dedifferentiation and their local release from electrospun PLGA fiber sheet can be applicable as a method to prevent intimal hyperplasia in stent, catheter, and vascular bypass and graft.

6. References

1. Kavanagh CA, Rochev YA, Gallagher WM, Dawson KA, Keenan AK. Local drug delivery in restenosis injury: thermoresponsive co-polymers as potential drug delivery systems. Pharmacol Ther 2004;102(1):1-15.
2. Fathi-Azarbayjani A, Chan SY. Single and Multi-Layered Nanofibers for Rapid and Controlled Drug Delivery. Chem Pharm Bull (Tokyo) 2010;58(2):143-6.
3. Musthaba SM, Baboota S, Ahmed S, Ahuja A, Ali J. Status of novel drug delivery technology for phytotherapeutics. Expert Opin Drug Deliv. 2009;6(6):625-37.
4. Chakraborty S, Liao IC, Adler A, Leong KW. Electrohydrodynamics: A facile technique to fabricate drug delivery systems. Adv Drug Deliv Rev 2009;61(12):1043-54.
5. Loo SC, Tan ZY, Chow YJ, Lin SL. Drug Release From Irradiated PLGA and PLLA Multi-Layered Films. J Pharm Sci 2010;99(7):3060-71.
6. Vert M, Schwach G, Engel R, Coudane J. Something new in the field of PLA/GA bioresorbable polymers?. J Control Release 1998;53:85-92.
7. Kim DW, Park YS, Kim YG, Piao H, Kwon JS, Hwang KK, et al. Local delivery of green tea catechins inhibits neointimal formation in the rat carotid artery injury model. Heart Vessels 2004;19(5):242-7.
8. Zou J, Huang Y, Cao K, Yang G, Yin H, Len J, et al. Effect of resveratrol on intimal hyperplasia after endothelial denudation in an experimental rabbit

model. Life Sci 2000;68(2):153-63.

9. Thakur RA, Florek CA, Kohn J, Michniak BB. Electrospun nanofibrous polymeric scaffold with targeted drug release profiles for potential application as wound dressing. Int J Pharm 2008;364(1):87-93.
10. Golomb G, Mayberg M, Domb AJ. Polymeric perivascular delivery systems. In: Domb AJ, editor. Polymeric site-specific pharmacotherapy. New York: John Wiley and Sons; 1994. p 205-19.
11. Golomb G, Moscovitz D, Fishbein I, Mishaly D. Perivascular polymeric controlled-release therapy. In: Wise DL, editor. Encyclopedic handbook of biomaterials and bioengineering. New York: Marcel Dekker; 1995. p 1043-55.
12. Signore PE, Machan LS, Jackson JK, Burt H, Bromley P, Wilson JE, et al. Complete inhibition of intimal hyperplasia by perivascular delivery of paclitaxel in ball oon-injured rat carotid arteries. J Vasc Interv Radiol 2001;12:79-88.
13. Fahrenholz M, Real R, Küken A, Saxena A, Orzechowski HD. Single low-dose administration of pharmacological inhibitor of mitogen-activated ERK kinase to the adventitia of the injured rat carotid artery suppresses neointima formation and inhibits nuclear ERK signaling. Eur J Pharmacol 2009;617(1-3):90-6.
14. Teomim D, Fishbein I, Golomb G, Orloff L, Mayberg M, Domb AJ. Perivascular delivery of heparin for the reduction of smooth muscle cell

proliferation after endothelial injury. J Control Rel 1999;60:129-42.

15. Edelman ER, Adams DH, Karnovsky MJ. Effect of controlled adventitial heparin delivery on smooth muscle cell proliferation following endothelial injury. Proc Natl Acad Sci USA 1990;87:3773-7.

16. Signore PE, Machan LS, Jackson JK, Burt H, Bromley P, Wilson JE, et al. Complete inhibition of intimal hyperplasia by perivascular delivery of paclitaxel in balloon-injured rat carotid arteries. J Vasc Interv Radiol 2001;12(1):79-88.

17. Barker SGE, Talbert A, Cottam S, Baskerville PA, Martin JF. Arterial intimal hyperplasia after occlusion of the adventitial vasa vasorum in the pig. Arterioscler Thromb Vasc Biol 1993;13:70–7.

18. Barker SGE, Tilling LC, Miller GC, Beesley JE, Fleetwood G, Stavri GT, et al. The adventitia and atherogenesis: removal initiates intimal proliferation in the rabbit which regresses on generation of a ‘neoadventitia’. Atherosclerosis 1994; 105:131–44.

19. Scott NA, Cipolla GD, Ross CE, Dunn B, Martin FH, Simonet L, et al. Identification of a potential role for the adventitia in vascular lesion formation after balloon overstretch injury of porcine coronary arteries. Circulation 1996;93:2178–87.

20. Zalewski A, Shi Y. Vascular myofibroblasts: lessons from coronary repairand remodelling. Arterioscler Thromb Vasc Biol 1997; 17:417– 22.

21. Shi Y, O’Brien JE, Ala-Kokko L, Chung W, Mannion JD, Zalewski A.

Origin of extracellular matrix synthesis during coronary repair. Circulation 1997; 95: 997–1006.

22. Wilcox JH, Waksman R, King SB, Scott NA. The role of adventitia in the arterial response to angioplasty: the effect of intravascular radiation. Int J Radiat Oncol Biol Phys 1996; 36:789–96.

23. Shi Y, Pieniek M, Fard A, O'Brien J, Mannion JD, Zalewski A. Adventitial remodeling after coronary arterial injury. Circulation 1996;93:340–8.

Abstract (in Korean)

소구경 인공혈관 이식 후 내막과형성증 방지를 위한 생리활성물질의 적용

(지도교수 박종철)

연세대학교 대학원 의과학과

이미희

내막과형성증은 동맥경화증, 혈관 성형술 및 혈관이식 등의 부분에서 관찰되는 만성적인 구조적 병변으로 과도한 조직의 성장을 유도한다. 이는 혈관 내벽 손상에 대한 반응으로, 혈관의 중막에서 혈관 평활근세포가 탈분화하여 이동 유도하여 내막으로 평활근 세포가 성장 함으로써 세포외기질이 생성되며 혈관내막이 두꺼워지게 된다. EGCG와 레스베라트롤은 항산화, 항증식, 항혈전 효과가 있으며, 심혈관 질환 예방 효과가 있다고 알려져 있다.

본 연구에서는 PDGF-bb (platelet-derived growth factor-bb)에 의해 탈분화 유도된 쥐의 대동맥 유래 평활근 세포(rat aorta smooth muscle cell)를 이용하여 천연 폴리페놀인 EGCG와 레스베라트롤의 탈분화 억제 효과를 세포 내 신호전달 경로의 탐색으로 확인하여 내막과형성 억제 기작에 대해 조사하였다. 또한, 전기방사법을 이용하여 이 두 물질을 PLGA 시트의 형태로 국소적인 약물 전달체를 제작하여, 풍선카테터를 이용해 혈관내막의 손상을 준 토끼의 복부동맥에

적용하여 내막과형성 억제효과를 확인하였다.

10 ng/ml의 PDGF-bb는 혈관 평활근 세포의 증식 및 세포주기의 진행을 유도하였고, 10분의 배양 후 PDGFR-β의인산화를 유도하여 4시간 까지 유지하였다. 또한 이의 발현으로 다음 경로인 42/44 MAPK, p38 MAPK, Akt의 인산화가 유도되었다. EGCG와 PDGF-bb를 혈청을 제거한 배지에 배양된 혈관 평활근 세포에 함께 처리하여 배양하였을 때 PDGF-bb에 의한 세포 증식을 EGCG의 농도 의존적으로 저해하였으며, 혈관 평활근 세포를 EGCG와 함께 24시간 동안 전처리 한 후, EGCG를 제거하여 PDGF-bb를 처리하였을 때 EGCG의 50 μM이상에서 세포성장을 억제하였다. 그리고 PDGF-bb에 의한 세포주기의 진행과 matrix metalloproteinases (MMP)의 생성도 EGCG에 의해 억제됨을 확인하였다. 50 μM의 EGCG와 전 처리된 혈관 평활근 세포는 PDGF-bb의 자극에 대한 PDGFR-β의 인산화를 저해하여 다음 신호전달체계의 인산화를 억제하였다. 또한 50 μM의 EGCG를 PDGF-bb와 함께 혈관 평활근 세포에 처리하였을 때, PDGFR-β의 인산화는 유도되지 않았고 다음 신호전달인 42/44 MAPK, p38 MAPK, Akt도 발현되지 않는 것을 확인하였다. EGCG는 직접 세포막에서 또는 PDGFR-β에서 PDGF-bb의 전달을 차단함으로써 세포 내 신호전달체계를 중단시켜 혈관 평활근 세포의 탈분화를 억제하는 것을 확인 할 수 있었다.

레스베라트롤은 농도 의존적으로 PDGF-bb에 의해 유도된 혈관 평활근 세포의 증식을 저해하였으며, 100 μM 이상의 농도에서 세포의 증식을 억제하였다. PDGF-bb는 혈관 평활근 세포의 탈분화를 유도하여 액틴 배열의 변화와 calponin과 αSMA의 발현을 저해시키고, 세포의 모양을 원의 형태로 변형시켰다. 반면, 20 μM의 resveratrol과 함께 배양 시 액틴이 한 방향으로 정열 하여 길게 늘어난 모양을

유지하고, calponin과 αSMA도 액틴이 배열된 위치에서 발현함을 확인하였다. 또한 100 μM의 레스베라트롤은 PDGF-bb 자극에 대해 세포내 신호전달체계 중 Akt와 다음 신호인 mTOR의 인산화를 억제하여 PDGF-bb에 의해 유도되는 신호전달체계의 균형을 방해하는 것을 확인하였다. 레스베라트롤은 PDGF-bb에 의한 세포내 신호전달체계를 불균형하게 하여 세포의 모양을 유지하고 세포의 증식을 저해할 수 있도록 세포의 탈분화를 억제함을 확인할 수 있었다.

전기방사법을 이용한 PLGA 섬유는 EGCG와 레스베라트롤의 존재여부와 상관없이 일정한 범위의 직경을 가지고 방울의 형성 없이 제작되었으며, EGCG와 레스베라트롤이 가지는 고유의 색인 적색과 노란색을 띄는 시트로 제작되었다. 또한 FT-IR 분석법을 통해 섬유와 시트에 각각의 물질이 존재함을 확인할 수 있었다. 각 물질이 함유된 PLGA 시트는 처음 넣은 양의 80~90%가 함유되어 있었다. 각 물질이 인산염완충 식염수(PBS, pH 7.4)에서 생분해성 고분자인 PLGA로부터 분비되는 양상을 비교해본 결과, EGCG를 포함하는 PLGA 시트는 잠입 하루 동안 초기 분비 양이 많았으며, 40일 동안 서서히 분비되었다. 레스베라트롤을 포함하는 PLGA 시트에서 레스베라트롤은 20일 동안 로그형태로 분비되었고, 잠입시간이 길어질수록 분비 양이 감소되었다. 제작된 시트는 혈관 내벽 손상 토끼모델을 이용하여 풍선 카테터에 의해서 손상된 복부동맥의 외부에 감싼 후 28일 동안 적용하여 내막과형성 억제효과를 확인하였다. 실험결과 EGCG 포함된 PLGA 시트를 적용한 군은 내막/중막의 비율이 PLGA 시트만 적용된 군보다 30% 감소하였으며, 레스베라트롤이 포함된 PLGA 시트가 적용된 군은 50% 감소효과를 확인할 수 있었다.

본 연구결과를 바탕으로, EGCG와 레스베라트롤은 혈관 평활근세포의 탈분화 예방을 위한 약물로의 사용 가능성이 있으며, 전기방사법으로 생분해성 고분자와 EGCG와 레스베라트롤을 이용해 만든 약물전달체는 내막과형성증 억제를 위한 치료에 활용가능성이 있음을 제시하였다.

핵심되는 말: 혈관 평활근세포, Epigallocatechin-3-O-gallate, 레스베라트롤, Platelet derived growth factor-bb, Platelet derived growth factor receptor-β, 탈분화, 세포 내 신호전달 체계, 내막과형성증, 전기방사, 약물전달시스템